Available online at www.sciencedirect.com
SCIENCE DIRECT®
Journal of Computational Physics 200 (2004) 549–580
JOURNAL OF COMPUTATIONAL PHYSICS
www.elsevier.com/locate/jcp

Discontinuous Galerkin methods for dispersive and lossy Maxwell's equations and PML boundary conditions

Tiao Lu [a], Pingwen Zhang [a], Wei Cai [b,*]

[a] *LMAM and School of Mathematical Science, Peking University, Beijing, 100871, PR China*
[b] *Department of Mathematics, University of North Carolina at Charlotte, Charlotte, NC 28223, USA*

Received 15 August 2003; received in revised form 17 February 2004; accepted 18 February 2004
Available online 21 July 2004

Abstract

In this paper, we will present a unified formulation of discontinuous Galerkin method (DGM) for Maxwell's equations in linear dispersive and lossy materials of Debye type and in the artificial perfectly matched layer (PML) regions. An auxiliary differential equation (ADE) method is used to handle the frequency-dependent constitutive relations with the help of auxiliary polarization currents in the computational and PML regions. The numerical flux for the dispersive lossy Maxwell's equations with the auxiliary polarization current variables is derived. Various numerical results are provided to validate the proposed formulation.

AMS: 65N30; 78A45

Keywords: Discontinuous Galerkin method; Electromagnetic scattering; Dispersive media; Riemann solver; UPML

1. Introduction

There has been active recent research in the development of discontinuous Galerkin methods (DGMs) for handling material interfaces arising from electromagnetic scattering [1–4]. The main advantages of the DGMs are the high order accuracy and parallel implementation as piecewise continuous approximation spaces are used to represent electromagnetic fields. The material interfaces are conformingly approximated in the underlying mesh triangulation of the solution domain. There are two approaches in implementing the DGMs, namely, the *h*-version and the *p*-version. Similar to the finite element methods [5], the *h*-version allows the mesh size to be decreased to achieve convergence at an order of the employed polynomial basis, resulting in a finite order method. The alternative *p*-version allows the order of the polynomials to be increased with the sizes of the elements kept at an initial triangulation. It will be shown in this paper, even

* Corresponding author. Tel.: +1-704-687-4581; fax: +1-704-687-6415.
E-mail address: wcai@uncc.edu (W. Cai).

0021-9991/$ - see front matter
doi:10.1016/j.jcp.2004.02.022

for discontinuous fields, exponential convergence with respect to the order of the basis functions can be obtained for DGM. A hybrid h–p version can also be considered [4].

An important aspect of time domain calculation of Maxwell's equations is the treatment of boundary conditions on the truncated computational domains. There are two popular ways of boundary treatment. The first kind is to define some kind of boundary operators (either differential or integral) so that no reflection occurs on the boundary, thus so-called non-reflective or absorbing boundary conditions [6–8]. The other kind of boundary treatment is to create a region of artificial absorbing layer around the computational domain so that waves, entering the artificial region transparently, will be attenuated within the region and the reflection back into the computational domain will be negligible and controllable. The second approach was initiated by Berenger's PML [9] and has attracted much research along this direction including the anitropic (Uniaxial) PML region [10,11]. The PML treatment of Berenger relies on the split field formulation of the Maxwell's equations in the PML region and has been shown in [12] to be only weakly stable. The uniaxial PML (UPML) proposed by Sacks and Ziolkowski does not require the splitting of the Maxwell's fields and is accomplished with the help of artificial polarization currents in the case of dispersive media. The resulting differential equations maintain the strong well-posedness of the original Maxwell's system [12].

In this paper, we will present a unified formulation of DGMs for the Maxwell's equations in both the computational and PML regions. To handle the frequency-dependent relation between the polarization P, M and the fields E, H, we use the auxiliary differential equation (ADE) method [13] to avoid the convolution-type constitutive relation in the time domain. The ADE method will be applicable in both the computational and PML regions. Several other issues will also be discussed such as the conservative form of the Maxwell's equations in both regions, definition of the polarization currents for the Debye media, and the construction of numerical fluxes based on the Riemann solutions.

The rest of the paper will be organized as follows. In Section 2, we introduce the Maxwell's equations in a linear dispersive and lossy media. A unified formulation of the Maxwell's equations with the added polarization currents will be introduced for both the computational and PML regions. The details of the derivation is provided in Appendix A. In Section 3, we give the discontinuous Galerkin discretization of the Maxwell's equations and numerical fluxes based on the Riemann solution of the Maxwell's equations with the added polarization current variables. In Section 4, numerical examples will be given to first verify the accuracy of the UPML boundary treatment for the DGM, then to validate the exponential convergence of the DGMs with the UPML boundary conditions, and finally to simulate the scattering of dispersive objects in lossy Debye media. A conclusion is given in Section 5 while appendices are included to give various technical derivations in the paper.

2. Maxwell's equations in Debye dispersive materials and PML regions

Maxwell's equations in MKS units are given in the general form as follows:

$$\frac{\partial \mathbf{D}}{\partial t} - \nabla \times \mathbf{H} = -\mathbf{J}, \tag{2.1}$$

$$\frac{\partial \mathbf{B}}{\partial t} + \nabla \times \mathbf{E} = 0, \tag{2.2}$$

where $\mathbf{E}$ and $\mathbf{H}$ are the macroscopic electric and magnetic fields, $\mathbf{D}$ and $\mathbf{B}$ are the electric displacement and magnetic induction fields, respectively, and $\mathbf{J}$ the current. The current, $\mathbf{J}$, is typically assumed to be related to the electric field, $\mathbf{E}$, through Ohm's law, $\mathbf{J} = \sigma \mathbf{E}$, where σ measures the finite conductivity of the medium.

In order to solve Maxwell's equations, we need the constitutive equations that relate $\mathbf{D}$ to $\mathbf{E}$ and $\mathbf{B}$ to $\mathbf{H}$, respectively

$$\mathbf{D} = \epsilon_0 \epsilon_{\mathrm{r},\infty} \mathbf{E} + \mathbf{P}, \tag{2.3}$$

$$\mathbf{B} = \mu_0 \mu_{\mathrm{r},\infty} \mathbf{H} + \mathbf{M}, \tag{2.4}$$

where ϵ_0 and μ_0 are the electric permittivity and the magnetic permeability of free space, $\epsilon_{\mathrm{r},\infty}$ and $\mu_{\mathrm{r},\infty}$ are the relative electric permittivity and the relative magnetic permeability of the medium at infinite frequency, and $\mathbf{P}$ and $\mathbf{M}$ are the electric polarization and the magnetic polarization, respectively.

In general, the components P_i of the electric polarization $\mathbf{P}$ are related to the components E_i of the electric field $\mathbf{E}$ via a power series in the frequency domain (indicated by $\breve{}$) as in Bloembergen [15]

$$\breve{P}_i = \epsilon_0 \sum_j \chi_{ij}(\omega) \breve{E}_j + \epsilon_0^2 \sum_{j,k} \chi_{ijk}(\omega) \breve{E}_j \breve{E}_k + \mathrm{O}(\breve{E}^3). \tag{2.5}$$

In linear and isotropic medium, the above relation is terminated at the first term to give

$$\breve{\mathbf{P}} = \epsilon_0 \chi(\omega) \breve{\mathbf{E}}, \tag{2.6}$$

where $\chi(\omega)$ is the electric susceptibility of the medium in frequency domain.

Here we assume that the magnetic polarization is 0, i.e., no magnetic effects are included in the treatment given here. The generalization of the relation between the magnetic polarization $\mathbf{M}$ and the magnetic field $\mathbf{H}$ can be made similarly.

For a single-pole Debye medium, the electric susceptibility in frequency domain can be expressed as

$$\chi(\omega) = \frac{\epsilon_{\mathrm{r,s}} - \epsilon_{\mathrm{r},\infty}}{1 + \mathrm{j}\omega\tau}, \tag{2.7}$$

where $\epsilon_{\mathrm{r,s}}$ is the static zero-frequency relative electric permittivity, and τ is the pole relation time.

The non-dimensionalized Maxwell's equations for linear dispersive and lossy materials and the artificial PML regions can be given in a unified form as follows. New auxiliary polarization currents $\mathbf{P}$, $\mathbf{Q}$s are introduced to decouple the frequency-dependent constitutive relations (2.3) and (2.6) (details of derivations are given in Appendices A and B). The non-dimensionalized Maxwell's equations for TM waves in dispersive media and in the UPML region are given as

$$\begin{aligned}
\epsilon_{\mathrm{r},\infty} \frac{\partial E_z}{\partial t} &= \frac{\partial H_y}{\partial x} - \frac{\partial H_x}{\partial y} - \left[\sigma + \epsilon_{\mathrm{r},\infty}(\sigma_x + \sigma_y) + \frac{\epsilon_{\mathrm{r,s}} - \epsilon_{\mathrm{r},\infty}}{\tau}\right] E_z + P_{z,1} + P_{z,2} - P_{z,3} - P_{z,4}, \\
\mu_{\mathrm{r}} \frac{\partial H_x}{\partial t} &= -\frac{\partial E_z}{\partial y} - \mu_{\mathrm{r}}(\sigma_y - \sigma_x) H_x + Q_x, \\
\mu_{\mathrm{r}} \frac{\partial H_y}{\partial t} &= \frac{\partial E_z}{\partial x} - \mu_{\mathrm{r}}(\sigma_x - \sigma_y) H_y + Q_y, \\
\frac{\partial P_{z,1}}{\partial t} &= -\epsilon_{\mathrm{r},\infty} \sigma_x \sigma_y E_z, \\
\frac{\partial P_{z,2}}{\partial t} &= -\frac{1}{\tau} P_{z,2} + \frac{\epsilon_{\mathrm{r,s}} - \epsilon_{\mathrm{r},\infty}}{\tau^2} E_z, \\
\frac{\partial P_{z,3}}{\partial t} &= -\frac{1}{\tau} P_{z,3} - \frac{\epsilon_{\mathrm{r,s}} - \epsilon_{\mathrm{r},\infty}}{\epsilon_{\mathrm{r},\infty}\tau} P_{z,1} + \frac{(\epsilon_{\mathrm{r,s}} - \epsilon_{\mathrm{r},\infty})(\sigma_x + \sigma_y)}{\tau} E_z, \\
\frac{\partial P_{z,4}}{\partial t} &= -\frac{\sigma}{\epsilon_{\mathrm{r},\infty}} P_{z,1} + \sigma(\sigma_x + \sigma_y) E_z, \\
\frac{\partial Q_x}{\partial t} &= -\sigma_x Q_x + \mu_{\mathrm{r}} \sigma_x (\sigma_y - \sigma_x) H_x, \\
\frac{\partial Q_y}{\partial t} &= -\sigma_y Q_y + \mu_{\mathrm{r}} \sigma_y (\sigma_x - \sigma_y) H_y,
\end{aligned} \tag{2.8}$$

where E_z is the z-component of the non-dimensionalized electric field, H_x and H_y are the x- and y-component of the non-dimensionalized magnetic field, respectively. Again, $\epsilon_{r,\infty}$ is the relative electric permittivity at infinite frequency, μ_r is the relative magnetic permeability. $\epsilon_{r,s}$ is the static zero-frequency relative electric permittivity, τ is the non-dimensionalized pole relaxation time, $P_{z,1}$, Q_x and Q_y are auxiliary variables introduced by the PML, $P_{z,2}$ is introduced by the medium dispersion, $P_{z,3}$ is introduced by the medium dispersion and the PML, $P_{z,4}$ is introduced by the medium loss and the PML. σ is the non-dimensionalized relative electric conductivity, σ_x and σ_y are the parameters for the PML. In the case that $\sigma_x = \sigma_y = 0$, the above equations reduce to the original Maxwell's equations in the physical dispersive region (2.1) and (2.2). Similar equations can be derived for the TE waves and will not be repeated here.

Setting $\mathbf{U} = (\epsilon_{r,\infty}E_z, \mu_r H_x, \mu_r H_y, P_{z,1}, P_{z,2}, P_{z,3}, P_{z,4}, Q_x, Q_y)^T$, the conservation form for the system is

$$\frac{\partial \mathbf{U}}{\partial t} + \nabla \cdot (\bar{\mathbb{A}}\mathbf{U}) = \mathbf{S}, \tag{2.9}$$

where $\bar{\mathbb{A}}$ and $\mathbf{S}$ will be given later. Note that the 4th–9th equations in Eq. (2.8) are all ordinary differential equations, we can rewrite the conservation system as

$$\frac{\partial \mathbf{U}^{(1)}}{\partial t} + \nabla \cdot (\mathbb{A}\mathbf{U}^{(1)}) = \mathbf{S}^{(1)}, \tag{2.10}$$

$$\frac{\partial \mathbf{U}^{(2)}}{\partial t} = \mathbf{S}^{(2)}, \tag{2.11}$$

where $\mathbf{U}^{(1)} = (\epsilon_{r,\infty}E_z, \mu_r H_x, \mu_r H_y)^T$, $\mathbf{U}^{(2)} = (P_{z,1}, P_{z,2}, P_{z,3}, P_{z,4}, Q_x, Q_y)^T$, $\mathbf{U} = (\mathbf{U}^{(1)}, \mathbf{U}^{(2)})^T$, $\mathbf{S} = (\mathbf{S}^{(1)}, \mathbf{S}^{(2)})^T$, and $\mathbb{A} = (A_x, A_y)$ and

$$A_x = \begin{pmatrix} 0 & 0 & -1/\mu_r \\ 0 & 0 & 0 \\ -1/\epsilon_{r,\infty} & 0 & 0 \end{pmatrix}, \quad A_y = \begin{pmatrix} 0 & 1/\mu_r & 0 \\ 1/\epsilon_{r,\infty} & 0 & 0 \\ 0 & 0 & 0 \end{pmatrix}.$$

And $\bar{\mathbb{A}}$ is given as

$$\bar{\mathbb{A}} = (\bar{A}_x, \bar{A}_y),$$

where

$$\bar{A}_x = \begin{pmatrix} A_x & 0_{3\times 6} \\ 0_{6\times 3} & 0_{6\times 6} \end{pmatrix}, \quad \bar{A}_y = \begin{pmatrix} A_y & 0_{3\times 6} \\ 0_{6\times 3} & 0_{6\times 6} \end{pmatrix}.$$

Here $0_{n\times m}$ denotes zero matrix with n rows and m columns. The source terms $\mathbf{S}^{(1)}$ and $\mathbf{S}^{(2)}$ represent body forces, e.g., currents,

$$\mathbf{S}^{(1)} = \begin{pmatrix} -\left[\sigma + \epsilon_{r,\infty}(\sigma_x + \sigma_y) + \frac{\epsilon_{r,s}-\epsilon_{r,\infty}}{\tau}\right]E_z + P_{z,1} + P_{z,2} - P_{z,3} - P_{z,4} \\ -\mu_r(\sigma_y - \sigma_x)H_x + Q_x \\ -\mu_r(\sigma_x - \sigma_y)H_y + Q_y \end{pmatrix}, \tag{2.12}$$

$$\mathbf{S}^{(2)} = \begin{pmatrix} -\epsilon_{r,\infty}\sigma_x\sigma_y E_z \\ -\frac{1}{\tau}P_{z,2} + \frac{\epsilon_{r,s}-\epsilon_{r,\infty}}{\tau^2}E_z \\ -\frac{1}{\tau}P_{z,3} - \frac{\epsilon_{r,s}-\epsilon_{r,\infty}}{\epsilon_{r,\infty}\tau}P_{z,1} + \frac{(\epsilon_{r,s}-\epsilon_{r,\infty})(\sigma_x+\sigma_y)}{\tau}E_z \\ -\frac{\sigma}{\epsilon_{r,\infty}}P_{z,1} + \sigma(\sigma_x + \sigma_y)E_z \\ -\sigma_x Q_x + \mu_r\sigma_x(\sigma_y - \sigma_x)H_x \\ -\sigma_y Q_y + \mu_r\sigma_y(\sigma_x - \sigma_y)H_y \end{pmatrix}. \tag{2.13}$$

3. DGMs for Maxwell's equations

Let $\mathscr{T}_h$ be a discretization of the solution domain Ω. For each element $K \in \mathscr{T}_h$, $\epsilon_{r,\infty}$ and μ_r are assumed constant on each element. We denote a finite-dimensional space of smooth functions defined on the element K by $\mathscr{P}(K)$. This space will be used to approximate the variable $\mathbf{U}$. Set

$$V_h := \{v \in L^1(\Omega) \,|\, v|_K \in \mathscr{P}(K) \ \forall K \in \mathscr{T}_h\} \tag{3.1}$$

and

$$V_h^9 := \underbrace{V_h \times V_h \times \cdots \times V_h}_{9}. \tag{3.2}$$

The DGM space discretization of the hyperbolic system for $\mathbf{U}$ can be written as follows: Find $\mathbf{U} \in V_h^9$ such that, for all $v_h \in V_h$

$$\int_K \left(\frac{\partial \mathbf{U}^{(1)}}{\partial t} v_h - \mathbf{S}^{(1)} v_h - \mathbb{A}\mathbf{U}^{(1)} \cdot \nabla v_h \right) \mathrm{d}\boldsymbol{x} + \int_{\partial K} \mathbf{h}_K(\mathbf{U}^{(1),-}, \mathbf{U}^{(1),+}) \cdot \hat{\boldsymbol{n}}_K v_h \,\mathrm{d}s = 0, \tag{3.3}$$

$$\int_K \left(\frac{\partial \mathbf{U}^{(2)}}{\partial t} v_h - \mathbf{S}^{(2)} v_h \right) \mathrm{d}\boldsymbol{x} = 0, \tag{3.4}$$

where $\hat{\boldsymbol{n}}_K = (n_x, n_y)$ is the outward unit normal to ∂K, $\mathbf{U}^{(1),-}$ and $\mathbf{U}^{(1),+}$ are defined as

$$\mathbf{U}^{(1),\pm}(\boldsymbol{x}) = \lim_{\delta \to 0^+} \mathbf{U}^{(1)}(\boldsymbol{x} \pm \delta \hat{\boldsymbol{n}}_k),$$

and the numerical flux $\mathbf{h}_K(\mathbf{U}^{(1),-}, \mathbf{U}^{(1),+})$ is an approximation to $\hat{\boldsymbol{n}}_K \cdot \mathbb{A}\mathbf{U}^{(1)}|_{\partial K}$ on the faces of the element K, and

$$\mathbf{h}_K(\mathbf{U}^{(1)}, \mathbf{U}^{(1)}) = \hat{\boldsymbol{n}}_K \cdot \mathbb{A}\mathbf{U}^{(1)}|_{\partial K}. \tag{3.5}$$

3.1. Numerical flux $\boldsymbol{h}_K(\boldsymbol{U}^{(I),-}, \boldsymbol{U}^{(I),+})$

From Eqs. (3.3) and (3.4), we can see that the numerical flux is only needed for $\mathbf{U}^{(1)}$, but not for $\mathbf{U}^{(2)}$. In the DGM, the computational domain Ω is composed of cells, or elements, K_i. On K_i, $\mathbf{U}$ is approximated by a linear combination of the basis functions and the approximation is not required to be continuous across ∂K_i. Therefore, for conservation, we have to replace $\int_{\partial K_i} \mathbb{A}\mathbf{U}^{(1)} \cdot \hat{\boldsymbol{n}} \,\mathrm{d}s$ with a numerical flux

$$\int_{\partial K_i} \mathbb{A} \cdot \hat{\boldsymbol{n}} \mathbf{U}^{(1)} \,\mathrm{d}s = \sum_{e \in \partial K_i, e = \Gamma_{ij}} \int_{\Gamma_{ij}} \mathbf{h}(\mathbf{U}^{(1),i}, \mathbf{U}^{(1),j}) \,\mathrm{d}s, \tag{3.6}$$

where the sum is taken over all the edges e of the cell, and $\partial K_i = \bigcup \Gamma_{ij}$, where $\Gamma_{ij} = K_i \cap K_j$, and $\hat{\boldsymbol{n}}$ is the outward unit normal vector to K_i. Note that the triangulation is assumed to satisfy the properties of finite-element triangulation: the K_i are non-overlapping sets and, if e is a given edge of ∂K_i, there exists a unique K_j such that $e = K_i \cup K_j$. $\mathbf{U}^{(1),i}$ is the field value local to the element K_i and $\mathbf{U}^{(1),j}$ is the field value local from the neighbour element K_j.

The flux $\mathbf{h}(\mathbf{U}^{(1),-}, \mathbf{U}^{(1),+})$ is defined by solving exactly or approximately a one-dimensional Riemann problem, in the direction $\hat{\boldsymbol{n}}$ normal to the edge $e = \Gamma_{ij}$. For this purpose, we define new variables ζ (normal) and τ (tangential) along the element edge

$$\zeta = n_x x + n_y y = \boldsymbol{x}\cdot\hat{\boldsymbol{n}}, \quad \tau = -n_y x + n_x y = \boldsymbol{x}\cdot\hat{\boldsymbol{n}}^{\perp}, \tag{3.7}$$

where $\hat{\boldsymbol{n}} = (n_x, n_y)$, $\hat{\boldsymbol{n}}^{\perp} = (-n_y, n_x)$ and $\boldsymbol{x} = (x, y)$. The system (2.10) and (2.11) is transformed into

$$\frac{\partial \tilde{\mathbf{U}}^{(1)}}{\partial t} + \frac{\partial}{\partial \zeta}(\mathbb{A}\cdot\hat{\boldsymbol{n}}\tilde{\mathbf{U}}^{(1)}) + \frac{\partial}{\partial \tau}(\mathbb{A}\cdot\hat{\boldsymbol{n}}^{\perp}\tilde{\mathbf{U}}^{(1)}) = \tilde{\mathbf{S}}^{(1)}, \tag{3.8}$$

$$\frac{\partial \tilde{\mathbf{U}}^{(2)}}{\partial t} = \tilde{\mathbf{S}}^{(2)}, \tag{3.9}$$

where

$$\tilde{\mathbf{U}}^{(l)}(\zeta,\tau,t) = \mathbf{U}^{(l)}(x(\zeta,\tau), y(\zeta,\tau), t), \quad \tilde{\mathbf{S}}^{(l)}(\zeta,\tau,t) = \mathbf{S}^{(l)}(x(\zeta,\tau), y(\zeta,\tau), t), \quad l = 1,2 \tag{3.10}$$

and

$$\mathbb{A}\cdot\hat{\boldsymbol{n}} = A_x n_x + A_y n_y, \quad \mathbb{A}\cdot\hat{\boldsymbol{n}}^{\perp} = -A_x n_y + A_y n_x. \tag{3.11}$$

The following shorthand notations are introduced

$$\tilde{\mathbf{U}} = (\tilde{\mathbf{U}}^{(1)}, \tilde{\mathbf{U}}^{(2)})^{\mathrm{T}}, \quad \tilde{\mathbf{S}} = (\tilde{\mathbf{S}}^{(1)}, \tilde{\mathbf{S}}^{(2)})^{\mathrm{T}}.$$

Now, if $\tilde{\mathbf{U}}^{(1)}$ is constant to each side of the line $\zeta = 0$, the associated Cauchy problem reduces to the one-dimensional Riemann problem along the direction $\hat{\boldsymbol{n}}$,

$$\frac{\partial}{\partial t}\tilde{\mathbf{U}}^{(1)} + \frac{\partial}{\partial \zeta}(\mathbb{A}\cdot\hat{\boldsymbol{n}}\tilde{\mathbf{U}}^{(1)}) = \tilde{\mathbf{S}}^{(1)}, \tag{3.12}$$

$$\frac{\partial}{\partial t}\tilde{\mathbf{U}}^{(2)} = \tilde{\mathbf{S}}^{(2)}, \tag{3.13}$$

$$\tilde{\mathbf{U}}(\zeta,0) = \begin{cases} \tilde{\mathbf{U}}^{-}, & \zeta < 0, \\ \tilde{\mathbf{U}}^{+}, & \zeta > 0 \end{cases} \tag{3.14}$$

and the flux $\mathbf{h}(\mathbf{U}^{(1),-}, \mathbf{U}^{(1),+})$ at the point is defined as $(\mathbb{A}\cdot\hat{\boldsymbol{n}}\tilde{\mathbf{U}}^{(1)})|_{\zeta=0}$. Here $(\mathbb{A}\cdot\hat{\boldsymbol{n}}\tilde{\mathbf{U}}^{(1)})|_{\zeta=0}$ means

$$(\mathbb{A}\cdot\hat{\boldsymbol{n}}\tilde{\mathbf{U}}^{(1)})|_{\zeta=0} = \lim_{t\to 0^+}\lim_{\zeta\to 0^-}\left(\mathbb{A}\cdot\hat{\boldsymbol{n}}\mathbf{U}^{(1)}(\zeta,t)\right) = \lim_{t\to 0^+}\lim_{\zeta\to 0^+}\left(\mathbb{A}\cdot\hat{\boldsymbol{n}}\mathbf{U}^{(1)}(\zeta,t)\right). \tag{3.15}$$

Only if the second equality in Eq. (3.15) holds, the definition of the numerical flux makes sense. In fact, from the Rankine–Hugoniot condition at the discontinuous line $\zeta = 0$, we can see that the second equality in Eq. (3.15) should hold.

Assume that the parameters $\epsilon_{\mathrm{r},\infty}^{-}$, $\epsilon_{\mathrm{r},\infty}^{+}$, μ_{r}^{-}, and μ_{r}^{+} are constant on each element and $\mathbb{A}\cdot\hat{\boldsymbol{n}}$ is discontinuous across $\zeta = 0$,

$$\mathbb{A}\cdot\hat{\boldsymbol{n}} = \begin{cases} \mathbb{A}^{-}\cdot\hat{\boldsymbol{n}}, & \zeta < 0, \\ \mathbb{A}^{+}\cdot\hat{\boldsymbol{n}}, & \zeta > 0, \end{cases} \tag{3.16}$$

where

$$\mathbb{A}^{\mp}\cdot\hat{\boldsymbol{n}} = \begin{pmatrix} 0 & n_y/\mu_{\mathrm{r}}^{\mp} & -n_x/\mu_{\mathrm{r}}^{\mp} \\ n_y/\epsilon_{\mathrm{r},\infty}^{\mp} & 0 & 0 \\ -n_x/\epsilon_{\mathrm{r},\infty}^{\mp} & 0 & 0 \end{pmatrix}. \tag{3.17}$$

So the numerical flux $\mathbf{h}_K(\mathbf{U}^{(1),-},\mathbf{U}^{(1),+})$ can be written as follows:

$$\mathbf{h}(\mathbf{U}^{(1),-},\mathbf{U}^{(1),+}) = \lim_{t\to 0^+}\left(\mathbb{A}^-\tilde{\mathbf{U}}^{(1)}(0^-,t)\right) = \lim_{t\to 0^+}\left(\mathbb{A}^+\tilde{\mathbf{U}}^{(1)}(0^+,t)\right), \tag{3.18}$$

where

$$\tilde{\mathbf{U}}^{(1)}(0^-,t) = \lim_{\zeta\to 0^-}\tilde{\mathbf{U}}^{(1)}(\zeta,t), \quad \tilde{\mathbf{U}}^{(1)}(0^+,t) = \lim_{\zeta\to 0^+}\tilde{\mathbf{U}}^{(1)}(\zeta,t). \tag{3.19}$$

The numerical flux $\mathbf{h}_K(\mathbf{U}^{(1),-},\mathbf{U}^{(1),+})$ for the Maxwell's equations can be shown as follows:

$$\tilde{\mathbf{h}}_K = \begin{pmatrix} -\hat{\boldsymbol{n}}_K \times \frac{(Z\mathbf{H}+\hat{\boldsymbol{n}}_K\times\mathbf{E})^- + (Z\mathbf{H}-\hat{\boldsymbol{n}}_K\times\mathbf{E})^+}{Z^-+Z^+} \\ \hat{\boldsymbol{n}}_K \times \frac{(Y\mathbf{E}-\hat{\boldsymbol{n}}_K\times\mathbf{H})^- + (Y\mathbf{E}+\hat{\boldsymbol{n}}_K\times\mathbf{H})^+}{Y^-+Y^+} \end{pmatrix}, \tag{3.20}$$

where $Z^\pm$ and $Y^\pm$ are the local impedance and admittance, respectively, and defined as

$$Z^\pm = \frac{1}{Y^\pm} = \sqrt{\frac{\mu_{\mathrm{r}}^\pm}{\epsilon_{\mathrm{r}}^\pm}}.$$

For TM_z wave, the numerical flux is given as (with details given in Appendix C)

$$\mathbf{h}_K(\mathbf{U}^{(1),-},\mathbf{U}^{(1),+}) = \begin{pmatrix} -\frac{\left[Z(n_xH_y-n_yH_x)-E_z\right]^- + \left[Z(n_xH_y-n_yH_x)+E_z\right]^+}{Z^-+Z^+} \\ n_y\frac{\left[YE_z-(n_xH_y-n_yH_x)\right]^- + \left[YE_z+(n_xH_y-n_yH_x)\right]^+}{Y^-+Y^+} \\ -n_x\frac{\left[YE_z-(n_xH_y-n_yH_x)\right]^- + \left[YE_z+(n_xH_y-n_yH_x)\right]^+}{Y^-+Y^+} \end{pmatrix}. \tag{3.21}$$

From the duality of the TE_z and TM_z cases, the numerical flux for the TE_z case can be obtained by replacing E_z with H_z, replacing H_x by $-E_x$, and replacing H_y by $-E_y$, replacing Z by Y and replacing Y by Z in Eq. (3.21),

$$\mathbf{h}_K(\mathbf{U}^{(1),-},\mathbf{U}^{(1),+}) = \begin{pmatrix} \frac{\left[Y(n_xE_y-n_yE_x)+H_z\right]^- + \left[Y(n_xE_y-n_yE_x)-H_z\right]^+}{Y^-+Y^+} \\ -n_y\frac{\left[ZH_z+(n_xE_y-n_yE_x)\right]^- + \left[ZH_z-(n_xE_y-n_yE_x)\right]^+}{Z^-+Z^+} \\ n_x\frac{\left[ZH_z+(n_xE_y-n_yE_x)\right]^- + \left[ZH_z-(n_xE_y-n_yE_x)\right]^+}{Z^-+Z^+} \end{pmatrix}. \tag{3.22}$$

where $\mathbf{U}^{(1)} = (\mu_{\mathrm{r},\infty}H_z, \epsilon_{\mathrm{r}}E_x, \epsilon_{\mathrm{r}}E_y)^{\mathrm{T}}$.

3.2. Mapping between the standard reference element and the physical element

We start by assuming that the computational domain, Ω, is decomposed into quadrilateral and triangular elements with straight or curved sides, as illustrated in Figs. 1 and 2.

The sides of the elements are not required be straight, but for most computational problems, the vast majority of the elements will have straight sides. We shall name the coordinates in the standard element I as $\xi = (\xi,\eta)$ while the coordinates in the physical element D as $\boldsymbol{x} = (x,y)$.

To relate operations in D to those in I, we need to construct a smooth and invertible mapping $\boldsymbol{\Psi} : D \to I$ that uniquely relates the physical elements and the standard reference elements. For curved triangles as in Fig. 3, a blending function can be constructed for the mapping [5]. In the case of Fig. 1, the mapping is

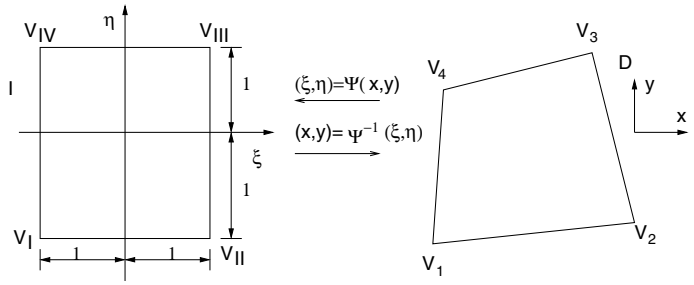

Fig. 1. Mapping between the quadrilateral D and the standard quadrilateral I.

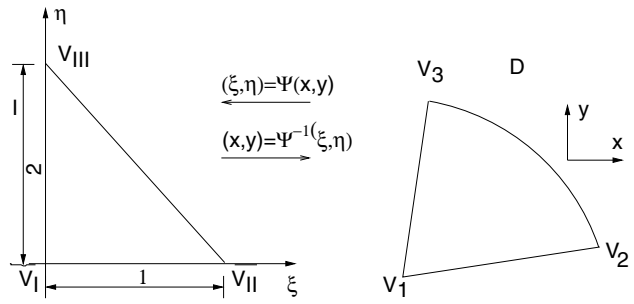

Fig. 2. Mapping between the curved triangle D and the standard triangle I.

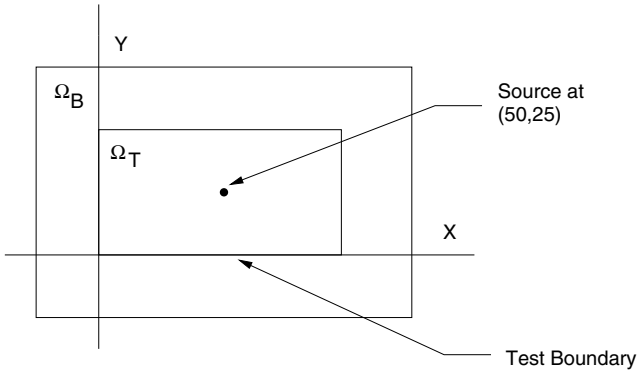

Fig. 3. Computational domains for testing reflectivity of boundary conditions.

$$\boldsymbol{x} = \boldsymbol{\Psi}(\boldsymbol{\xi}) = \frac{(1-\xi)(1-\eta)}{4} v_1 + \frac{(1+\xi)(1-\eta)}{4} v_2 + \frac{(1+\xi)(1+\eta)}{4} v_3 + \frac{(1-\xi)(1+\eta)}{4} v_4, \tag{3.23}$$

where v_1, v_2, v_3, and v_4 are the coordinates of the vertexes V_1, V_2, V_3, and V_4, respectively.

Once the mapping $\boldsymbol{\Psi}(\boldsymbol{\xi})$ has been established, we can use it to compute the curvilinear metric of the transformation by

$$\frac{\partial \boldsymbol{x}}{\partial \boldsymbol{\xi}}\frac{\partial \boldsymbol{\xi}}{\partial \boldsymbol{x}} = \begin{pmatrix} x_\xi & x_\eta \\ y_\xi & y_\eta \end{pmatrix}\begin{pmatrix} \xi_x & \xi_y \\ \eta_x & \eta_y \end{pmatrix} = \begin{pmatrix} 1 & 0 \\ 0 & 1 \end{pmatrix}. \tag{3.24}$$

With this new metric, the derivative of a function, $u = u(x, y)$, is expressed

$$\frac{\partial u}{\partial x} = \frac{\partial u}{\partial \xi}\frac{\partial \xi}{\partial x} + \frac{\partial u}{\partial \eta}\frac{\partial \eta}{\partial x}.$$

And $\partial u/\partial y$ can be similarly expressed.

Consider a smooth function, $f[D] \in C[D]$ for which $f(\boldsymbol{x}) : D \to R$. The integration on the physical element D is computed by the following formulation:

$$\int_D f(\boldsymbol{x})\,\mathrm{d}\boldsymbol{x} = \int_I Jf(\boldsymbol{x}(\boldsymbol{\xi}))\,\mathrm{d}\boldsymbol{\xi}, \tag{3.25}$$

where J is the transformation Jacobian

$$J = \left|\frac{\partial \boldsymbol{x}}{\partial \boldsymbol{\xi}}\right|.$$

In addition to the integration for the element D, the integration over the sides of the element D needs to be computed, too. Once the mapping $\boldsymbol{\Psi}$ has been established, the mappings between the sides of the physical element and the sides of the reference element can also be derived. The integration on one of the side, $\overline{V_1V_2}$, of the physical element D is computed by

$$\int_{\overline{V_1V_2}} f(\boldsymbol{x})\,\mathrm{d}\mathbf{s} = \int_{\overline{V_1V_{\mathrm{II}}}} J_1 f(\boldsymbol{x}(\boldsymbol{\xi}))\,\mathrm{d}\mathbf{s}', \tag{3.26}$$

where J_1 is the Jacobian of the transformation relating the side $\overline{V_1V_2}$ of the physical element D to the side $\overline{V_1V_{\mathrm{II}}}$ of the reference element I.

3.3. A multivariate polynomial basis on the standard reference element

First, we construct a set of basis functions on the standard reference element I, then using the mapping $\boldsymbol{\Psi}$, we can obtain a set of basis functions on the physical element D. For example, we can define a set of basis functions on the standard reference element I in Fig. 1 or 2:

$$P_n^2 = \mathrm{span}\{\xi^i\eta^j; i, j \geqslant 0; i + j \leqslant n\} = \mathrm{span}\{\phi_j\}_{j=1}^N,$$

where n signifies the maximum order of the polynomial and $N = ((n + 2)(n + 1))/2$. And the corresponding set of basis functions on the physical element D are

$$\mathrm{span}\{\xi^i(x, y)\eta^j(x, y); i, j \geqslant 0; i + j \leqslant n\},$$

where $(\xi, \eta) = \boldsymbol{\Psi}^{-1}(x, y)$.

A set of basis functions for the standard rectangle element can be chosen as

$$\mathrm{span}\{L_i(\xi)L_j(\eta); i, j \geqslant 0; i + j \leqslant n\} = \mathrm{span}\{\phi_j\}_{j=1}^N,$$

where $L_i(\cdot)$ is the Legendre polynomial of order i and $N = ((n + 2)(n + 1))/2$. And the set of basis functions on each element D is obtained by the mapping $\boldsymbol{\Psi}$. For triangular elements, if higher order basis ($n > 7$) is desired, Dubinar orthogonal polynomial basis functions have been shown to provide well-conditioned mass matrices (3.34) and yield exponential convergence for even discontinuous fields [16].

3.4. Space discretization

With the function basis and the flux defined, we can formulate the DGM for Maxwell's equations, Eqs. (2.10) and (2.11). First, we assume that the electric field E_z, and magnetic field H_x and H_y are represented in terms of the basis functions $\phi_j(\boldsymbol{x})$,

$$E_{z,N}(\boldsymbol{x},t)=\sum_{j=1}^{N}E_{z,j}\phi_j(\boldsymbol{x}),$$

$$H_{x,N}(\boldsymbol{x},t)=\sum_{j=1}^{N}H_{x,j}\phi_j(\boldsymbol{x}),$$

$$H_{y,N}(\boldsymbol{x},t)=\sum_{j=1}^{N}H_{y,j}\phi_j(\boldsymbol{x})$$

within each general curvilinear element D. Here $E_{z,j}$ and $H_{x,j}$, $H_{y,j}$ are the time-dependent coefficients and $\phi_j(\boldsymbol{x})$ is the jth basis function. And $\mathbf{U}^{(2)}$ is also projected to the function space expanded by the basis functions,

$$P_{z,s,N}(\boldsymbol{x},t)=\sum_{j=1}^{N}P_{z,s,j}\phi_j(\boldsymbol{x}),\quad s=1,2,3,4,$$

$$Q_{t,N}(\boldsymbol{x},t)=\sum_{j=1}^{N}Q_{t,j}\phi_j(\boldsymbol{x}),\qquad t=x,y.$$

We shall require that the equation, Eq. (3.3), be satisfied in the following way:

$$\int_D\left(\frac{\partial\mathbf{U}_N^{(1)}}{\partial t}\phi_i(\boldsymbol{x})-\mathbf{S}_N^{(1)}\phi_i(\boldsymbol{x})-\mathbb{A}\cdot\nabla\phi_i(\boldsymbol{x})\right)\mathrm{d}\boldsymbol{x}+\int_{\partial\mathrm{D}}\mathbf{h}_D(\mathbf{U}_N^{(1),-},\mathbf{U}_N^{(1),+})\phi_i(x)\,\mathrm{d}s=0,\tag{3.27}$$

where $\mathbf{U}_N^{(1)}$, $\mathbf{h}_D(\mathbf{U}_N^{(1),-},\mathbf{U}_N^{(1),+})$, and $\mathbf{S}_N^{(1)}=(S_N^{E_z},S_N^{H_x},S_N^{H_y})^{\mathrm{T}}$ refer to the approximate state vector, flux, and body force, respectively. $\mathbf{U}_N^{(1),-}$ is the approximate field value local to the element D, and $\mathbf{U}_N^{(1),+}$ is the approximate field value from the neighbor element. $\mathbf{h}_D=(h_D^{E_z},h_D^{H_x},h_D^{H_y})^{\mathrm{T}}$ is the numerical flux. $S_N^l(\boldsymbol{x},t)=\sum_{j=1}^{N}S_j^l\phi_j(\boldsymbol{x})$, $l=E_z,H_x,H_y$, where $S_j^l,S_j^{H_x},S_j^{H_y}$ are the time-dependent coefficients.

Also, Eq. (3.4) is satisfied in the following way:

$$\int_D\left(\frac{\partial\mathbf{U}_N^{(2)}}{\partial t}\phi_i(\boldsymbol{x})-\mathbf{S}_N^{(2)}\phi_i(\boldsymbol{x})\right)\mathrm{d}\boldsymbol{x}=0,\tag{3.28}$$

where $\mathbf{U}_N^{(2)}$ and $\mathbf{S}_N^{(2)}$ refer to the approximate state vector, and body force, respectively.

Assuming that $\epsilon_{\mathrm{r},\infty},\mu_{\mathrm{r}},\sigma_x,\sigma_y,\tau,\sigma$ be constant on each element, Eqs. (3.27) and (3.28) can be written as

$$\sum_{j=1}^{N}\left(\epsilon_{\mathrm{r},\infty}M_{ij}\frac{\mathrm{d}E_{z,j}}{\mathrm{d}t}+M_{ij}^{x}H_{y,j}-M_{ij}^{y}H_{x,j}\right)+\int_{\partial D}h_D^{E_z}(\mathbf{U}_N^{(1),-},\mathbf{U}_N^{(1),+})\phi_i(x)\,\mathrm{d}s=\sum_{j=1}^{N}M_{ij}S_j^{E_z},\tag{3.29}$$

where

$$S_j^{E_z} = -\left[\sigma + \epsilon_{\mathrm{r},\infty}(\sigma_x + \sigma_y) + \frac{\epsilon_{\mathrm{r,s}} - \epsilon_{\mathrm{r},\infty}}{\tau}\right] E_{z,j} + P_{z,1,j} + P_{z,2,j} - P_{z,3,j} - P_{z,4,j},$$

$$\sum_{j=1}^{N}\left(\mu_{\mathrm{r}} M_{ij}\frac{\mathrm{d}H_{x,j}}{\mathrm{d}t} - M_{ij}^{y}E_{z,j}\right) + \int_{\partial D} h_D^{H_x}(\mathbf{U}_N^{(1),-}, \mathbf{U}_N^{(1),+})\phi_i(x)\,\mathrm{d}s = \sum_{j=1}^{N} M_{ij}S_j^{H_x}, \tag{3.30}$$

where

$$S_j^{H_x} = -\mu_{\mathrm{r}}(\sigma_y - \sigma_x)H_{x,j} + Q_{x,j},$$

$$\sum_{j=1}^{N}\left(\mu_{\mathrm{r}} M_{ij}\frac{\mathrm{d}H_{y,j}}{\mathrm{d}t} + M_{ij}^{x}E_{z,j}\right) + \int_{\partial D} h_D^{H_y}(\mathbf{U}_N^{(1),-}, \mathbf{U}_N^{(1),+})\phi_i(x)\,\mathrm{d}s = \sum_{j=1}^{N} M_{ij}S_j^{H_y}, \tag{3.31}$$

where

$$S_j^{H_y} = -\mu_{\mathrm{r}}(\sigma_x - \sigma_y)H_{y,j} + Q_{y,j},$$

$$\sum_{j=1}^{N}\left(M_{ij}\frac{\mathrm{d}P_{z,1,j}}{\mathrm{d}t} + \epsilon_{\mathrm{r},\infty}\sigma_x\sigma_y M_{ij}E_{z,j}\right) = 0, \tag{3.32}$$

$$\vdots$$

$$\sum_{j=1}^{N}\left(M_{ij}\frac{\mathrm{d}Q_{y,j}}{\partial t} + \sigma_y M_{ij}Q_{y,j} - \mu_{\mathrm{r}}\sigma_y(\sigma_x - \sigma_y)M_{ij}H_{y,j}\right) = 0. \tag{3.33}$$

Here we have introduced the local mass matrix

$$M_{ij} = \int_{\mathrm{D}} \phi_i(\boldsymbol{x})\phi_j(\boldsymbol{x})\,\mathrm{d}\boldsymbol{x} \tag{3.34}$$

and two local stiffness matrices

$$M_{ij}^{x} = \int_D \frac{\partial\phi_i(\boldsymbol{x})}{\partial x}\phi_j(\boldsymbol{x})\,\mathrm{d}\boldsymbol{x},$$

$$M_{ij}^{y} = \int_D \frac{\partial\phi_i(\boldsymbol{x})}{\partial y}\phi_j(\boldsymbol{x})\,\mathrm{d}\boldsymbol{x}.$$

After introducing the following notations:

$$\mathbf{E}^z = (E_{z,1}, E_{z,2}, \ldots, E_{z,N})^{\mathrm{T}}, \quad \mathbf{H}^x = (H_{x,1}, H_{x,2}, \ldots, H_{x,N})^{\mathrm{T}},$$

$$\mathbf{H}^y = (H_{y,1}, H_{y,2}, \ldots, H_{y,N})^{\mathrm{T}}, \quad \boldsymbol{\phi} = (\phi_1, \phi_2, \ldots, \phi_N)^{\mathrm{T}}$$

Eqs. (3.29)–(3.33) read explicitly

$$\frac{\mathrm{d}\mathbf{E}^z}{\mathrm{d}t} = -(\epsilon_{\mathrm{r},\infty}M)^{-1}M^x\mathbf{H}^y + (\epsilon_{\mathrm{r},\infty}M)^{-1}M^y\mathbf{H}^x - (\epsilon_{\mathrm{r},\infty}M)^{-1}\int_{\partial D} h_D^{E_z}(\mathbf{U}_N^{(1),-},\mathbf{U}_N^{(1),+})\boldsymbol{\phi}(x)\,\mathrm{d}s + \frac{1}{\epsilon_{\mathrm{r},\infty}}\mathbf{S}_N^{E_z}, \quad (3.35)$$

where

$$\mathbf{S}_N^{E_z} = (S_1^{E_z}, S_2^{E_z}, \ldots, S_N^{E_z})^{\mathrm{T}},$$

$$\frac{\mathrm{d}\mathbf{H}^x}{\mathrm{d}t} = (\mu_{\mathrm{r}}M)^{-1}M^y\mathbf{E}^z - (\mu_{\mathrm{r}}M)^{-1}\int_{\partial D} h_D^{H_x}(\mathbf{U}_N^{(1),-},\mathbf{U}_N^{(1),+})\boldsymbol{\phi}(x)\,\mathrm{d}s + \frac{1}{\mu_{\mathrm{r}}}\mathbf{S}_N^{H_x}, \quad (3.36)$$

where

$$\mathbf{S}_N^{H_x} = (S_1^{H_x}, S_2^{H_x}, \ldots, S_N^{H_x})^{\mathrm{T}},$$

$$\frac{\mathrm{d}\mathbf{H}^y}{\mathrm{d}t} = -(\mu_{\mathrm{r}}M)^{-1}M^x\mathbf{E}^z - (\mu_{\mathrm{r}}M)^{-1}\int_{\partial D} h_D^{H_y}(\mathbf{U}_N^{(1),-},\mathbf{U}_N^{(1),+})\boldsymbol{\phi}(x)\mathrm{d}s + \frac{1}{\mu_{\mathrm{r}}}\mathbf{S}_N^{H_y}, \quad (3.37)$$

where

$$\mathbf{S}_N^{H_y} = (S_1^{H_y}, S_2^{H_y}, \ldots, S_N^{H_y})^{\mathrm{T}},$$

$$\frac{\mathrm{d}P_{z,1,j}}{\mathrm{d}t} = -\epsilon_{\mathrm{r},\infty}\sigma_x\sigma_y E_{z,j}, \quad (3.38)$$

$$\vdots$$

$$\frac{\mathrm{d}Q_{y,j}}{\mathrm{d}t} = -\sigma_y Q_{y,j} + \mu_{\mathrm{r}}\sigma_y(\sigma_x - \sigma_y)H_{y,j}. \quad (3.39)$$

Eqs. (3.35)–(3.39) are ordinary equations and will be solved by Runge–Kutta methods.

4. Numerical results

4.1. Validation of the UPML boundary conditions for the DGM

To validate the accuracy of the proposed UPML boundary conditions, we consider a standard test problem [14,13] to simulate an outgoing cylindrical wave generated by a hard source inside the computational domain. Fig. 3 shows two domains ($\Omega_T \subset \Omega_B$) on which both FDTD algorithm and the DGM will be used and compared for the calculation of a TM_z wave.

For a given numerical algorithm and a specific boundary treatment, we make two independent calculations, first we compute the scattering field, denoted by E_z^B, of the hard source on the bigger domain Ω_B with zero boundary condition on $\partial\Omega_B$ (Ω_B is chosen to be large enough so no reflection will come into Ω_T within the duration of the computation time). Second, we compute the solution E_z^T on the smaller test domain Ω_T with the specific boundary condition imposed on $\partial\Omega_T$. Then, we define the difference at mesh point $(i,j) \in \Omega_T$ between the two solutions as the reflection error caused by the specific boundary condition,

$$D(i,j) = E_z^T(i,j) - E_z^B(i,j). \quad (4.1)$$

The second-order Yee's finite difference scheme is used to test the accuracy of the Mur absorbing boundary condition (ABC) while the DGM to test the accuracy of the UPML boundary treatment. The general second-order absorbing boundary condition [14] at the left grid boundary of Ω_T is given by

$$\frac{\partial^2}{\partial x \partial t} U - \frac{p_0}{c} \frac{\partial^2}{\partial t^2} U + c p_2 \frac{\partial^2}{\partial y^2} U = 0, \tag{4.2}$$

where U is the component of the electric field E_z, c is the velocity of the light in the free space. The choice of the coefficients p_0 and p_2 in (4.2) produces various families of absorbing boundary conditions. With $p_0 = 1$ and $p_2 = -0.5$, (4.2) corresponds to the Mur ABC [13]. The ABCs at the other boundaries of Ω_T are similar to Eq. (4.2).

In the Yee's scheme, a global reflected error is defined as

$$E = \sum_{(i,j) \in \Omega_T} D^2(i,j), \tag{4.3}$$

which measures the total reflected error within the test domain at a given time step. For the DGM, the global reflected error is defined by,

$$E = \sum_{K_{i,j} \subset \Omega_T} \frac{1}{|K_{i,j}|} \int_{K_{i,j}} (E_z^T - E_z^B)^2 \, \mathrm{d}x \, \mathrm{d}y. \tag{4.4}$$

Similar mesh sizes are used for both Yee's scheme and the DGM. The local reflection error was obtained at the first row of the grid points away from the boundary $y = 0$. Fig. 4 compares the local error due to the second-order Mur ABC and 10-cell PML boundary treatment (with a reflection factor (4.17) $R(0) = \mathrm{e}^{-16}$). The local error was scaled by the maximum absolute value of E_z. Fig. 4 shows that the local error due the UPML is on the order of $10^{-9} \times$ Mur ABC, i.e., 180 dB below the Mur ABC. Fig. 5 is the global error for both the Mur ABC and the PML ABC, which shows that the global error due to the PML is on the order of $10^{-10} \times$ Mur ABC, i.e., 100 dB below the Mur ABC.

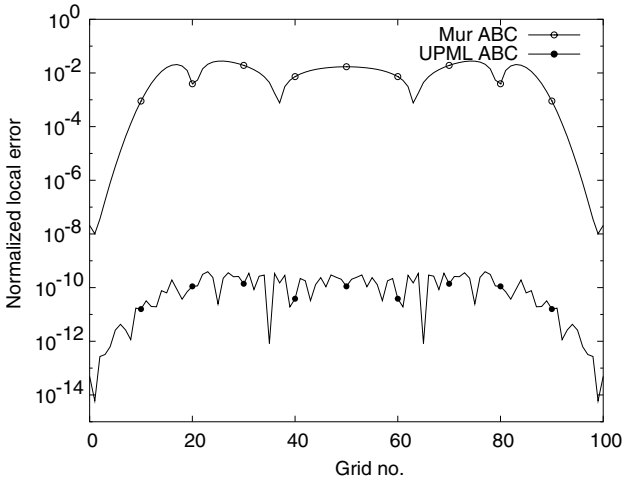

Fig. 4. Local E_z error at time-step $n = 100$ for both the second-order Mur ABC and a 10-cell cubic graded UPML, plotted on a logarithmic vertical scale.

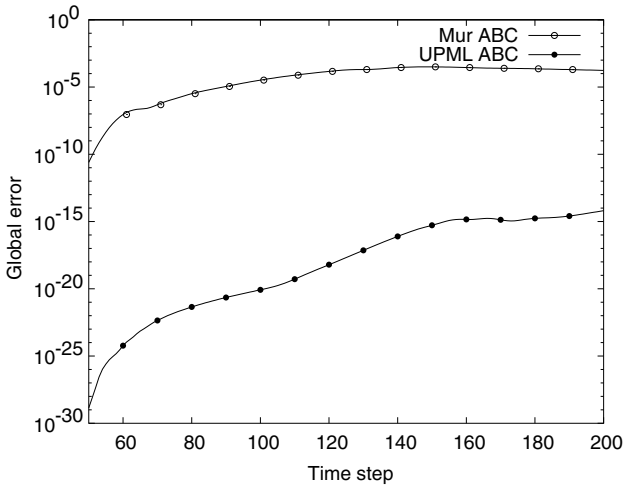

Fig. 5. Global error for both the second-order Mur ABC and a 10-cell cubic graded UPML, plotted as a function of time-step number on a logarithmic vertical scale.

4.2. Exponential convergence for TE and TM scattering of a dielectric cylinder

As high order basis functions can be used in the DGMs, we expect the convergence rate will be exponential with respect to the order of basis functions. In this example, we will demonstrate such an exponential convergence of the DGMs for the scattering of a dielectric cylinder.

We will consider both the TM and TE scattering, for the two-dimensional TM wave, we have the Maxwell's equations

$$\epsilon_{\mathrm{r}} \frac{\partial E_z}{\partial t} = \frac{\partial H_y}{\partial x} - \frac{\partial H_x}{\partial y}, \tag{4.5}$$

$$\mu_{\mathrm{r}} \frac{\partial H_x}{\partial t} = -\frac{\partial E_z}{\partial y}, \tag{4.6}$$

$$\mu_{\mathrm{r}} \frac{\partial H_y}{\partial t} = \frac{\partial E_z}{\partial x}, \tag{4.7}$$

subject to boundary conditions between two regions with material parameters, ϵ_k and μ_k, for $k = 1,2$, as

$$E_z^{(1)} = E_z^{(2)}, \tag{4.8}$$

$$\hat{\boldsymbol{n}} \times \mathbf{H}^{(1)} = \hat{\boldsymbol{n}} \times \mathbf{H}^{(2)}. \tag{4.9}$$

Here $\mathbf{H}^k = (H_x^{(k)}, H_y^{(k)}, 0)$, $k = 1,2$ and $\hat{\boldsymbol{n}} = (n_x, n_y, 0)$ represents a unit normal to the material interface. Similar equations can be written for the TE case and are omitted here.

We assume that the cylinder with radius $r_0 = 0.6$, $\epsilon_2 = 2.25$, $\mu_2 = 2$ embedded in the free space is illuminated by a TM time-harmonic incident plane wave of the form

$$E_z^{\mathrm{i}} = \cos(k_0 x - \omega t), \quad H_y^{\mathrm{i}} = -\cos(k_0 x - \omega t), \tag{4.10}$$

where the propagation constant for homogeneous, isotropic free-space medium $k_0 = \omega\sqrt{\mu_0 \epsilon_0}$.

We will use the scattering wave formulation

$$\epsilon_{\mathrm{r}} \frac{\partial E_z^{\mathrm{s}}}{\partial t} = \frac{\partial H_y^{\mathrm{s}}}{\partial x} - \frac{\partial H_x^{\mathrm{s}}}{\partial y} - (\epsilon_{\mathrm{r}} - \epsilon_{\mathrm{r}}^{\mathrm{i}}) \frac{\partial E_z^{\mathrm{i}}}{\partial t}, \tag{4.11}$$

$$\mu_{\mathrm{r}} \frac{\partial H_x^{\mathrm{s}}}{\partial t} = -\frac{\partial E_z^{\mathrm{s}}}{\partial y} - (\mu_{\mathrm{r}} - \mu_{\mathrm{r}}^{\mathrm{i}}) \frac{\partial H_x^{\mathrm{i}}}{\partial t}, \tag{4.12}$$

$$\mu_{\mathrm{r}} \frac{\partial H_y^{\mathrm{s}}}{\partial t} = \frac{\partial E_z^{\mathrm{s}}}{\partial x} - (\mu_{\mathrm{r}} - \mu_{\mathrm{r}}^{\mathrm{i}}) \frac{\partial H_y^{\mathrm{i}}}{\partial t}. \tag{4.13}$$

For the TE excitation, we choose the cylinder's parameters to be $\epsilon_2 = 2$ and $\mu_2 = 1.96$. The incident plane wave is set to be

$$H_z^{\mathrm{i}} = \cos(k_0 x - \omega t), \quad E_y^{\mathrm{i}} = \cos(k_0 x - \omega t). \tag{4.14}$$

4.2.1. Exact boundary conditions

With the angular frequency $\omega = 2\pi$, we first use the exact series solution [18] as the boundary conditions and initial conditions. Temporal integration of the semi-discretized approximation given in Eqs. (3.35)–(3.39) is done using a $(n+1)$th order (n is the order of the polynomial of the basis functions) or fourth-order Runge–Kutta method if $n \geqslant 3$. The time step used in the computation is taken heuristically to be

$$\Delta t = \mathrm{CFL} \min_{\Omega} \sqrt{\epsilon_{\mathrm{r}} \mu_{\mathrm{r}}} h, \tag{4.15}$$

with $\sqrt{\epsilon_{\mathrm{r}} \mu_{\mathrm{r}}}$ being the modified local speed of light due to materials, h is the minimum mesh size (the minimum length of the sides), and CFL typically takes values of $1/(2n+1)$. More rigorous criteria for the selection of the time steps for unstructured meshes can be found in [23].

We can see the exponential convergence with increasing order of the approximation n in Fig. 6 for a fixed mesh.

4.2.2. PML boundary treatment

Next we will show the effect of PML boundary treatment on the accuracy of the DGM. The finite element triangularization is shown in Fig. 7. The UPML losses $\sigma_x(x)$ is set to be polynomial profile [13],

$$\sigma_x(x) = (l/d)^m \sigma_{x,\max}, \tag{4.16}$$

where l is the distance from the interface between the PML and the physical solution domain, and d is the thickness of the PML. The definition of $\sigma_y(y)$ is similar. Eq. (4.16) increases the value of the PMLs σ_x from zero at $l = 0$, the surface of the PML, to $\sigma_{x,\max}$ at $l = d$, the PEC outer boundary. The reflection factor is

$$R(\theta) = \mathrm{e}^{-2\eta \sigma_{x,\max} d \epsilon_{\mathrm{r},\infty} \cos\theta/(m+1)}, \tag{4.17}$$

where η is the PMLs characteristic wave impedance and θ is the incident angle. For polynomial grading, the PML parameters can be readily determined for a given error estimate. For example, let m, d, and the desired reflection error $R(0)$ be known, $\sigma_{x,\max}$ can be computed as

$$\sigma_{x,\max} = -\frac{(m+1)\ln(R(0))}{2\eta d \epsilon_{\mathrm{r},\infty}}. \tag{4.18}$$

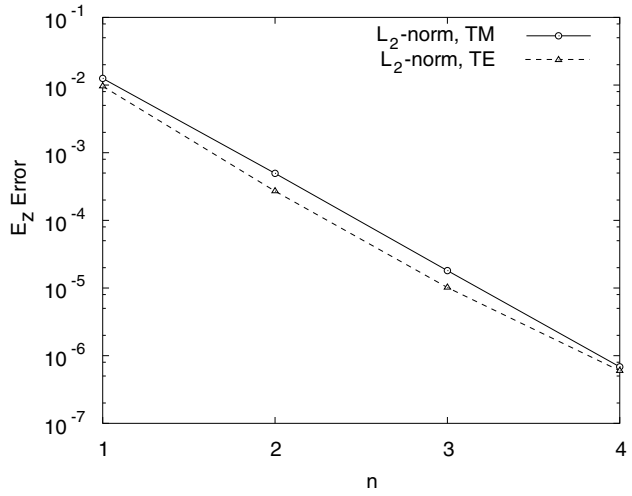

Fig. 6. Exponential decay of the L_2-norm of the error of E_z with increasing order of approximation, n. The exact boundary condition is used.

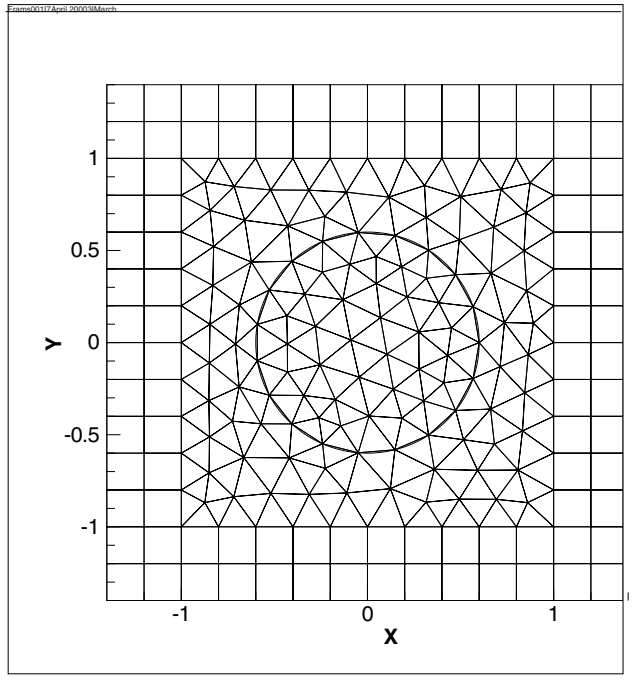

Fig. 7. Triangularization of the initial computational domain $[-1,1]^2$ containing a circle of radius 0.6 centered at (0,0) and a PML region.

Again, we see the exponential convergence with increasing order of the approximation n in a semi-log plot Fig. 8 for a different fixed mesh with a 10 cell PML region (with a reflection factor (4.17) $R(0) = e^{-16}$). However, it should be noted that once the reflection errors from the PML layers dominate the discreti-

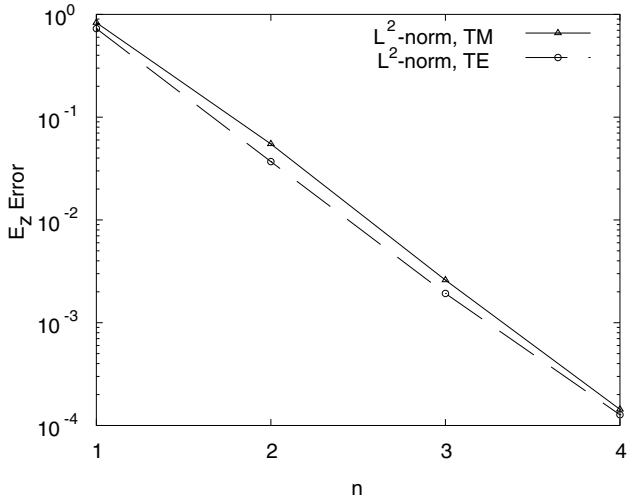

Fig. 8. Exponential decay of the L_2-norm of the error of E_z with respect to the order of the basis function n. A 10 cell UPML is used to terminate the computational domain.

zation errors of the DGM, the exponential convergence will not continue. Meanwhile, Figs. 9–11 show the contour of the TM scattering wave H_x, H_y and E_z using the fourth order of approximation, respectively.

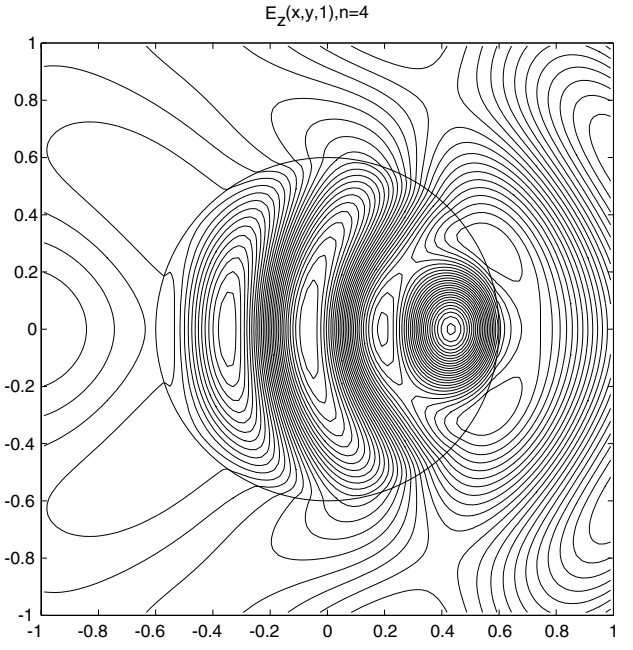

Fig. 9. The contour of the scattered E_z with the order of approximation, $n = 4$.

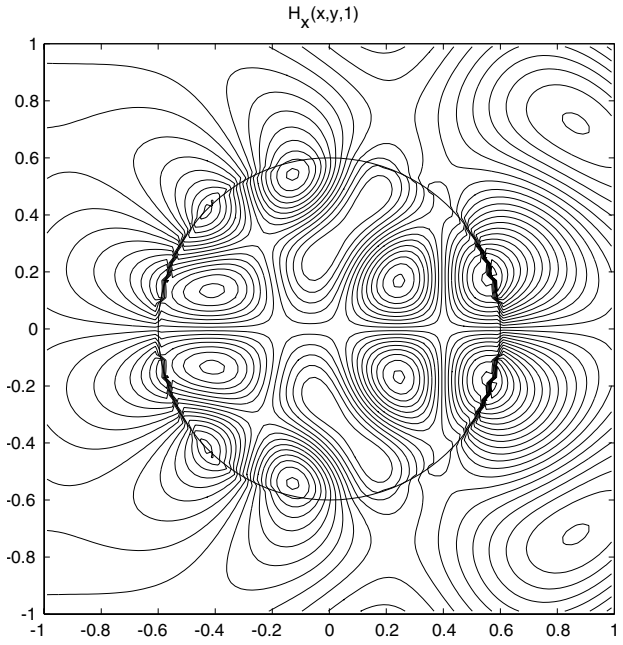

Fig. 10. The contour of the scattered H_x with the order of approximation, $n = 4$.

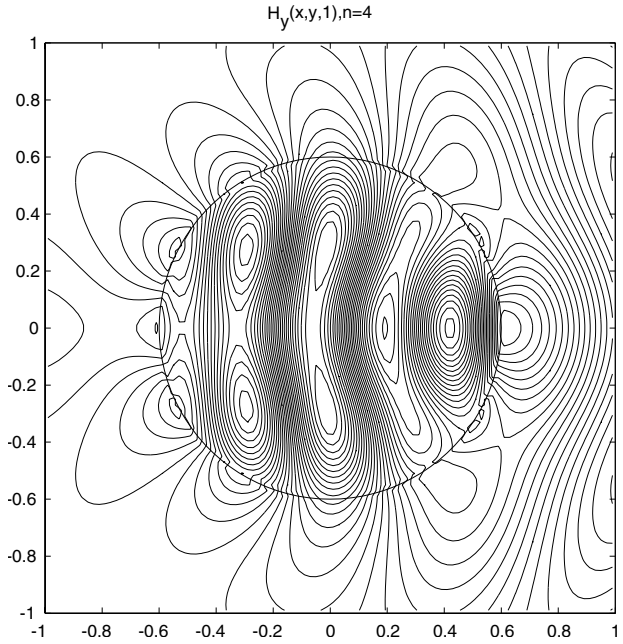

Fig. 11. The contour of the scattered H_y with the order of approximation, $n = 4$.

Remark. We would like to discuss the divergence free property of the proposed DGM, the method does not impose the divergence free condition explicitly in the design of the method. However, our numerical results have shown that the magnitude for the divergence of the magnetic field for TM case or the electric field for TE case remains at the level of the initial data. Fig. 12 shows the exponential convergence of zero divergence of the magnetic field on a semi-log plot.

There has some recent work on using divergence free basis function in each individual elements, thus eliminating one of the sources of the divergence error [22].

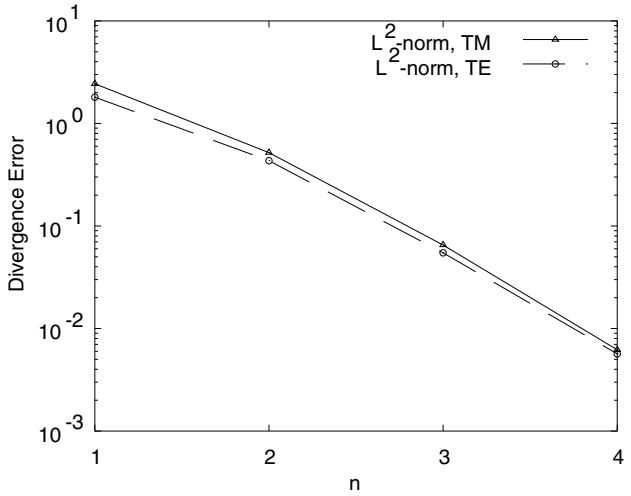

Fig. 12. Exponential decay of the L_2-norm of the divergence error of magnetic field with respect to the order of the basis function n. A 10 cell UPML is used to terminate the computational domain.

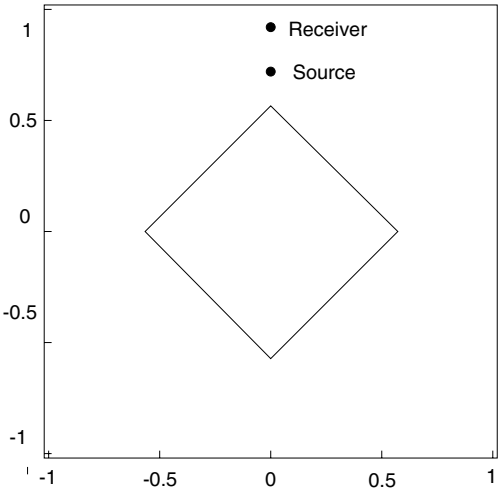

Fig. 13. A dispersive rotated square cylinder.

4.3. Scattering by a dispersive square cylinder

To demonstrate the proposed unified formulation of the DGM for dispersive and PML regions, we will compute the scattered field from a dispersive square cylinder illustrated in Fig. 13. All units are non-dimensionalized in this example. We will consider two types of dispersive media: Medium I: $\epsilon_{r,\infty} = 4$, $\epsilon_{r,s} = 12$, $\sigma = 0.002$ S/m, $\tau = 2.0 \times 10^{-10}$, Medium II: $\epsilon_{r,\infty} = 9$, $\epsilon_{r,s} = 16$, $\sigma = 0.004$ S/m, $\tau = 6.4 \times 10^{-11}$ The cylinder is of Debye Medium II and the background is a medium of Medium I [19]. The geometry of the cylinder and the locations of the source and receiver are shown in Fig. 13. The source locates at $(0.0, 0.72)$ in the center of a rectangular element, and the receiver locates at $(0.0, 0.92)$. The time step $\Delta t = 0.002$. The triangle mesh is generated with the shortest side of the resulting mesh being 0.028. The PML region has a width of 10 cells.

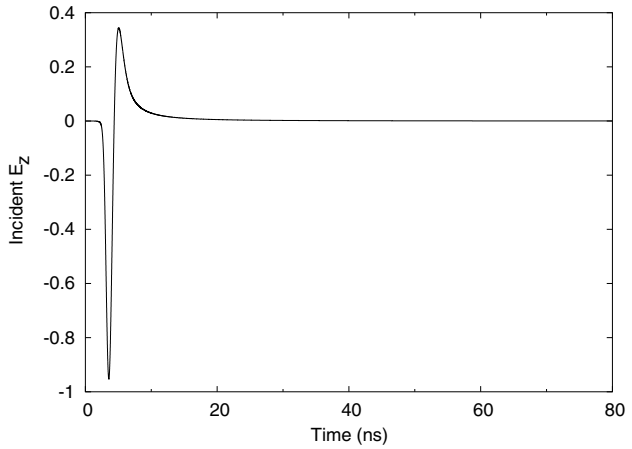

Fig. 14. Incident field at the receiver as a function of time and the background is Medium I.

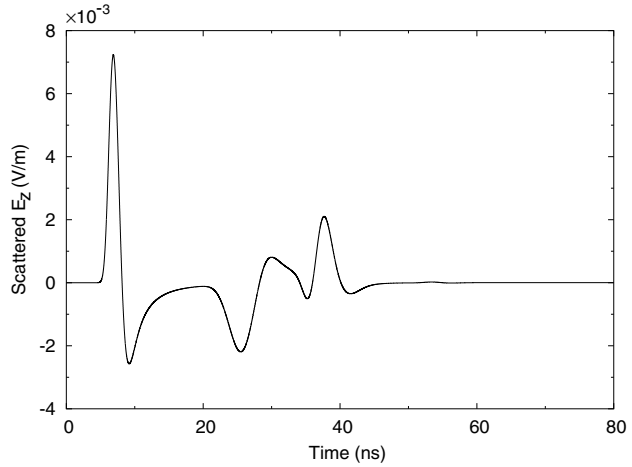

Fig. 15. Scattered field at the receiver as a function of time of a rotated square cylinder and the background is Medium I.

We select the source to be an electric current source in z-direction (J_z), which is the following Gaussian pulse:

$$J_z(t) = \exp\left(-\left(\frac{t-t_0}{t_{\text{decay}}}\right)^2\right), \tag{4.19}$$

where $t_0 = 0.54$, $t_{\text{decay}} = t_0/4$, and $f_c = 5/3$.

Fig. 14 shows the incident field E_z^{i} as a function of time in the absence of the square cylinder. When the dispersive cylinder is present, we calculate the total field. By subtracting the incident field from the total field, we obtain in Fig. 15 the scattered field E_z^{s} as a function of time.

5. Conclusion

We have presented a unified formulation of DGMs for Maxwell's equations in a linear dispersive and lossy Debye materials and in the artificial PML regions. Numerical results demonstrate the excellent performance of the PML layer with the DGM, and also the exponential convergence of the DGM even for discontinuous solutions provided that the errors from the PML layers do not dominate the errors from the discontinuous Galerkin discretization.

Acknowledgements

The work of Zhang was partially supported by National Science Foundation of China 90207009 and for Distinguished Young Scholars 10225103 while the work of Cai is supported partially by the US National Science Foundation (Grant Nos. CCR-9972251, CCR-9988375, CCR-0098140 and CCR-0098275).

Appendix A. Unified formulation of Maxwell's equations in dispersive media and UPML region

Consider an inhomogeneous, conductive and electrically dispersive medium with magnetic relative permeability μ_{r} and conductivity σ. A general time-harmonic form of Maxwell's equations in a dispersive medium or a UPML can be written as

$$\nabla \times \breve{\mathbf{H}} = \mathrm{j}\omega\epsilon_0\left(\epsilon_{\text{r}} + \frac{\sigma}{\mathrm{j}\omega\epsilon_0}\right)\bar{\bar{\epsilon}}\breve{\mathbf{E}}, \tag{A.1}$$

$$\nabla \times \breve{\mathbf{E}} = -\mathrm{j}\omega\mu_0\mu_{\text{r}}\bar{\bar{\mu}}\breve{\mathbf{H}}, \tag{A.2}$$

where

$$\bar{\bar{\epsilon}} = \bar{\bar{\mu}} = \begin{bmatrix} \frac{s_y s_z}{s_x} & 0 & 0 \\ 0 & \frac{s_x s_z}{s_y} & 0 \\ 0 & 0 & \frac{s_x s_y}{s_z} \end{bmatrix} \tag{A.3}$$

and

$$s_i = 1 + \frac{\sigma_i}{\mathrm{j}\omega\epsilon_0}, \quad i = x, y, z. \tag{A.4}$$

ϵ_0 and μ_0 are the permittivity and permeability of free space, respectively, and ϵ_r is the relative permittivity of the dispersive media. $\sigma_i = 0$ corresponds to the original physical dispersive medium. We consider two important classes of material dispersions: the Debye relaxation and the Lorentzian resonance. These two cases are now defined using the $\exp(j\omega t)$ time convention for phasor quantities (cf. [13, pp. 374–375]). For a Debye medium having P poles, we have

$$\epsilon_r(\omega) = \epsilon_{r,\infty} + \sum_{p=1}^{P} \frac{\epsilon_{r,s,p} - \epsilon_{r,\infty,p}}{1 + j\omega\tau_p}, \tag{A.5}$$

where $\epsilon_{r,s,p}$ is the static zero-frequency relative permittivity, $\epsilon_{r,\infty}$ is the relative permittivity at infinite frequency due to the pth Debye pole, and τ_p is the pth pole relaxation time.

For a Lorentz medium having P pole pairs, we have

$$\epsilon_r(\omega) = \epsilon_{r,\infty} + \sum_{p=1}^{P} \frac{(\epsilon_{r,s,p} - \epsilon_{r,\infty,p})\omega_p^2}{\omega_p^2 + 2j\omega\delta_p - \omega^2}, \tag{A.6}$$

where ω_p is the frequency of the pth Lorentz pole pair (the undamped resonant frequency of the medium) and δ_p is the damping coefficient.

In this paper, we will give the formulation for the Debye medium. Let the relative permittivity with a single pole be

$$\epsilon_r(\omega) = \epsilon_{r,\infty} + \frac{\epsilon_{r,s} - \epsilon_{r,\infty}}{1 + j\omega\tau}. \tag{A.7}$$

For simplicity, we just consider the 2D TM_z case ($s_z = 1$), the Maxwell's equations for TM_z wave for the Debye medium having a single pole can be written as

$$\frac{\partial \breve{H}_y}{\partial x} - \frac{\partial \breve{H}_x}{\partial y} = j\omega\epsilon_0 \left(\epsilon_{r,\infty} + \frac{\epsilon_{r,s} - \epsilon_{r,\infty}}{1 + j\omega\tau} + \frac{\sigma}{j\omega\epsilon_0} \right) s_x s_y \breve{E}_z, \tag{A.8}$$

$$\frac{\partial \breve{E}_z}{\partial y} = -j\omega\mu_0\mu_r \frac{s_y}{s_x} \breve{H}_x, \tag{A.9}$$

$$-\frac{\partial \breve{E}_z}{\partial x} = -j\omega\mu_0\mu_r \frac{s_x}{s_y} \breve{H}_y. \tag{A.10}$$

Eq. (A.8) can be written as

$$\frac{\partial \breve{H}_y}{\partial x} - \frac{\partial \breve{H}_x}{\partial y} = j\omega\epsilon_0\epsilon_{r,\infty} \breve{E}_z + \sigma \breve{E}_z + \breve{J}_{z,1}(\omega) + \breve{J}_{z,2}(\omega) + \breve{J}_{z,3}(\omega) + \breve{J}_{z,4}(\omega), \tag{A.11}$$

where

$$\breve{J}_{z,1}(\omega) = j\omega\epsilon_0\epsilon_{r,\infty}(s_x s_y - 1)\breve{E}_z, \tag{A.12}$$

$$\breve{J}_{z,2}(\omega) = j\omega\epsilon_0 \frac{\epsilon_{r,s} - \epsilon_{r,\infty}}{1 + j\omega\tau} \breve{E}_z, \tag{A.13}$$

$$\breve{J}_{z,3}(\omega) = \mathrm{j}\omega\epsilon_0 \frac{\epsilon_{\mathrm{r,s}} - \epsilon_{\mathrm{r},\infty}}{1 + \mathrm{j}\omega\tau}(s_x s_y - 1)\breve{E}_z = (s_x s_y - 1)\breve{J}_{z,2}(\omega) = \frac{\epsilon_{\mathrm{r,s}} - \epsilon_{\mathrm{r},\infty}}{\epsilon_{\mathrm{r},\infty}(1 + \mathrm{j}\omega\tau)}\breve{J}_{z,1}(\omega), \tag{A.14}$$

$$\breve{J}_{z,4}(\omega) = \sigma(s_x s_y - 1)\breve{E}_z = \frac{\sigma}{\mathrm{j}\omega\epsilon_0\epsilon_{\mathrm{r},\infty}}\breve{J}_{z,1}(\omega). \tag{A.15}$$

After substituting s_x and s_y from Eq. (A.4), we have

$$\begin{aligned}\breve{J}_{z,1}(\omega) &= \mathrm{j}\omega\epsilon_0\epsilon_{\mathrm{r},\infty}\left(\left(1 + \frac{\sigma_x}{\mathrm{j}\omega\epsilon_0}\right)\left(1 + \frac{\sigma_y}{\mathrm{j}\omega\epsilon_0}\right) - 1\right)\breve{E}_z = \mathrm{j}\omega\epsilon_0\epsilon_{\mathrm{r},\infty}\left(\frac{\sigma_x + \sigma_y}{\mathrm{j}\omega\epsilon_0} + \frac{\sigma_x\sigma_y}{(\mathrm{j}\omega\epsilon_0)^2}\right)\breve{E}_z \\ &= \epsilon_{\mathrm{r},\infty}(\sigma_x + \sigma_y)\breve{E}_z + \frac{\epsilon_{\mathrm{r},\infty}}{\mathrm{j}\omega\epsilon_0}\sigma_x\sigma_y\breve{E}_z,\end{aligned} \tag{A.16}$$

$$\breve{J}_{z,2}(\omega) = \mathrm{j}\omega\epsilon_0 \frac{\epsilon_{\mathrm{r,s}} - \epsilon_{\mathrm{r},\infty}}{1 + \mathrm{j}\omega\tau}\breve{E}_z, \tag{A.17}$$

$$\breve{J}_{z,3}(\omega) = \frac{\epsilon_{\mathrm{r,s}} - \epsilon_{\mathrm{r},\infty}}{\epsilon_{\mathrm{r},\infty}(1 + \mathrm{j}\omega\tau)}\breve{J}_{z,1}, \tag{A.18}$$

$$\breve{J}_{z,4}(\omega) = \frac{\sigma}{\mathrm{j}\omega\epsilon_0\epsilon_{\mathrm{r},\infty}}\breve{J}_{z,1}. \tag{A.19}$$

Now considering Eq. (A.11), we apply the inverse Fourier transform using the identity $\mathrm{j}\omega f(\omega) \to (\partial/\partial t)f(t)$. This yields an equivalent equation of time-domain differential equation for Eq. (A.11)

$$\frac{\partial H_y}{\partial x} - \frac{\partial H_x}{\partial y} = \epsilon_0\epsilon_{\mathrm{r},\infty}\frac{\partial E_z}{\partial t} + \sigma E_z + J_{z,1}(t) + J_{z,2}(t) + J_{z,3}(t) + J_{z,4}(t). \tag{A.20}$$

Next we will derive dynamic equations for (A.16)–(A.19). The way to obtain a dynamic equation for $J_{z,1}$ from Eq. (A.16) is to first multiply both sides of this equation by $(\mathrm{j}\omega)$, which gives

$$\mathrm{j}\omega\breve{J}_{z,1} = \mathrm{j}\omega\epsilon_{\mathrm{r},\infty}(\sigma_x + \sigma_y)\breve{E}_z + \frac{\epsilon_{\mathrm{r},\infty}}{\epsilon_0}\sigma_x\sigma_y\breve{E}_z. \tag{A.21}$$

Exploiting the differentiation theorem for the Fourier transform, we perform an inverse Fourier transform of each term in Eq. (A.21)

$$\frac{\partial J_{z,1}(t)}{\partial t} = \epsilon_{\mathrm{r},\infty}(\sigma_x + \sigma_y)\frac{\partial E_z}{\partial t} + \frac{\epsilon_{\mathrm{r},\infty}}{\epsilon_0}\sigma_x\sigma_y E_z. \tag{A.22}$$

To obtain the dynamic equation for $J_{z,2}$ from Eq. (A.17), we again multiply both sides of this equation by $(1 + \mathrm{j}\omega\tau)$,

$$\breve{J}_{z,2} + \mathrm{j}\omega\tau\breve{J}_{z,2} = \mathrm{j}\omega\epsilon_0(\epsilon_{\mathrm{r,s}} - \epsilon_{\mathrm{r},\infty})\breve{E}_z. \tag{A.23}$$

Similarly, using the inverse Fourier transform, we get

$$J_{z,2} + \tau\frac{\partial J_{z,2}}{\partial t} = \epsilon_0(\epsilon_{\mathrm{r,s}} - \epsilon_{\mathrm{r},\infty})\frac{\partial E_z}{\partial t}, \tag{A.24}$$

and by the same token, from (A.18) and (A.19) we have

$$J_{z,3} + \tau \frac{\partial J_{z,3}}{\partial t} = \frac{\epsilon_{r,s} - \epsilon_{r,\infty}}{\epsilon_{r,\infty}} J_{z,1}, \tag{A.25}$$

$$\frac{\partial J_{z,4}}{\partial t} = \frac{\sigma}{\epsilon_0 \epsilon_{r,\infty}} J_{z,1}. \tag{A.26}$$

(A.22), (A.24)–(A.26) are the time domain differential equations for all J_zs.

Next, we will further simplify the differential equations for the polarization currents J_zs so that they will become simply ordinary differential equations as shown in (2.8).

Considering Eq. (A.22), introduce a new parameter

$$P_{z,1} = -J_{z,1} + \epsilon_{r,\infty}(\sigma_x + \sigma_y) E_z. \tag{A.27}$$

Then Eq. (A.22) can be written as

$$\frac{\partial P_{z,1}}{\partial t} = -\frac{\epsilon_{r,\infty}}{\epsilon_0} \sigma_x \sigma_y E_z. \tag{A.28}$$

Similarly for Eq. (A.24), introducing a new parameter

$$P_{z,2} = -J_{z,2} + \frac{\epsilon_0(\epsilon_{r,s} - \epsilon_{r,\infty})}{\tau} E_z, \tag{A.29}$$

we have

$$\frac{\partial P_{z,2}}{\partial t} = \frac{1}{\tau} J_{z,2}. \tag{A.30}$$

From Eqs. (A.27) and (A.29), we can get

$$J_{z,1} = -P_{z,1} + \epsilon_{r,\infty}(\sigma_x + \sigma_y) E_z \tag{A.31}$$

and

$$J_{z,2} = -P_{z,2} + \frac{\epsilon_0(\epsilon_{r,s} - \epsilon_{r,\infty})}{\tau} E_z. \tag{A.32}$$

Now, after substituting for $J_{z,1}$ and $J_{z,2}$ from Eqs. (A.31) and (A.32) into Eq. (A.20), we have

$$\begin{aligned} \frac{\partial H_y}{\partial x} - \frac{\partial H_x}{\partial y} &= \epsilon_0 \epsilon_{r,\infty} \frac{\partial E_z}{\partial t} + \sigma E_z - P_{z,1} + \epsilon_{r,\infty}(\sigma_x + \sigma_y) E_z - P_{z,2} + \frac{\epsilon_0(\epsilon_{r,s} - \epsilon_{r,\infty})}{\tau} E_z + J_{z,3}(t) + J_{z,4}(t) \\ &= \epsilon_0 \epsilon_{r,\infty} \frac{\partial E_z}{\partial t} + \left[\sigma + \epsilon_{r,\infty}(\sigma_x + \sigma_y) + \frac{\epsilon_0(\epsilon_{r,s} - \epsilon_{r,\infty})}{\tau} \right] E_z - P_{z,1} - P_{z,2} + J_{z,3} + J_{z,4}. \end{aligned} \tag{A.33}$$

Next considering Eq. (A.30), after substituting for $J_{z,2}$ from Eq. (A.32), we have

$$\frac{\partial P_{z,2}}{\partial t} = -\frac{1}{\tau} P_{z,2} + \frac{\epsilon_0(\epsilon_{r,s} - \epsilon_{r,\infty})}{\tau^2} E_z. \tag{A.34}$$

Similarly for Eq. (A.25), after substituting for $J_{z,1}$ from Eq. (A.31), we have

$$\begin{aligned}\frac{\partial J_{z,3}}{\partial t} &= -\frac{1}{\tau}J_{z,3} + \frac{\epsilon_{\mathrm{r,s}} - \epsilon_{\mathrm{r},\infty}}{\epsilon_{\mathrm{r},\infty}\tau}\left[-P_{z,1} + \epsilon_{\mathrm{r},\infty}(\sigma_x + \sigma_y)E_z\right] \\ &= -\frac{1}{\tau}J_{z,3} - \frac{\epsilon_{\mathrm{r,s}} - \epsilon_{\mathrm{r},\infty}}{\epsilon_{\mathrm{r},\infty}\tau}P_{z,1} + \frac{(\epsilon_{\mathrm{r,s}} - \epsilon_{\mathrm{r},\infty})(\sigma_x + \sigma_y)}{\tau}E_z. \end{aligned} \tag{A.35}$$

Finally, for Eq. (A.26), after substituting for $J_{z,1}$ from Eq. (A.31), we have

$$\frac{\partial J_{z,4}}{\partial t} = -\frac{\sigma}{\epsilon_0\epsilon_{\mathrm{r},\infty}}P_{z,1} + \frac{\sigma(\sigma_x + \sigma_y)}{\epsilon_0}E_z. \tag{A.36}$$

Similar operations can be done to Faraday's Law equations (A.9) and (A.10), and we have the following equations:

$$\frac{\partial E_z}{\partial y} = -\mu_0\mu_{\mathrm{r}}\frac{\partial H_x}{\partial t} - \mu_0\mu_{\mathrm{r}}\frac{\sigma_y - \sigma_x}{\epsilon_0}H_x + Q_x, \tag{A.37}$$

$$-\frac{\partial E_z}{\partial x} = -\mu_0\mu_{\mathrm{r}}\frac{\partial H_y}{\partial t} - \mu_0\mu_{\mathrm{r}}\frac{\sigma_x - \sigma_y}{\epsilon_0}H_y + Q_y, \tag{A.38}$$

$$\frac{\partial Q_x}{\partial t} = -\frac{\sigma_x}{\epsilon_0}Q_x + \frac{\mu_0\mu_{\mathrm{r}}\sigma_x(\sigma_y - \sigma_x)}{\epsilon_0^2}H_x, \tag{A.39}$$

$$\frac{\partial Q_y}{\partial t} = -\frac{\sigma_y}{\epsilon_0}Q_y + \frac{\mu_0\mu_{\mathrm{r}}\sigma_y(\sigma_x - \sigma_y)}{\epsilon_0^2}H_y. \tag{A.40}$$

For consistency of notations, we let $P_{z,3} = J_{z,3}$ and $P_{z,4} = J_{z,4}$, then from Eqs. (A.33), (A.37), (A.38), (A.28), (A.34), (A.35), (A.36), (A.39) and (A.40), we get a new set of equations for E_z, H_x, H_y, $P_{z,1}$, $P_{z,2}$, $P_{z,3}$, $P_{z,4}$, Q_x, Q_y as follows:

$$\epsilon_0\epsilon_{\mathrm{r},\infty}\frac{\partial E_z}{\partial t} = \frac{\partial H_y}{\partial x} - \frac{\partial H_x}{\partial y} - \left[\sigma + \epsilon_{\mathrm{r},\infty}(\sigma_x + \sigma_y) + \frac{\epsilon_0(\epsilon_{\mathrm{r,s}} - \epsilon_{\mathrm{r},\infty})}{\tau}\right]E_z + P_{z,1} + P_{z,2} - P_{z,3} - P_{z,4}, \tag{A.41}$$

$$\mu_0\mu_{\mathrm{r}}\frac{\partial H_x}{\partial t} = -\frac{\partial E_z}{\partial y} - \mu_0\mu_{\mathrm{r}}\frac{\sigma_y - \sigma_x}{\epsilon_0}H_x + Q_x, \tag{A.42}$$

$$\mu_0\mu_{\mathrm{r}}\frac{\partial H_y}{\partial t} = \frac{\partial E_z}{\partial x} - \mu_0\mu_{\mathrm{r}}\frac{\sigma_x - \sigma_y}{\epsilon_0}H_y + Q_y, \tag{A.43}$$

$$\frac{\partial P_{z,1}}{\partial t} = -\frac{\epsilon_{\mathrm{r},\infty}}{\epsilon_0}\sigma_x\sigma_y E_z, \tag{A.44}$$

$$\frac{\partial P_{z,2}}{\partial t} = -\frac{1}{\tau}P_{z,2} + \frac{(\epsilon_{\mathrm{r,s}} - \epsilon_{\mathrm{r},\infty})}{\tau^2}E_z, \tag{A.45}$$

$$\frac{\partial P_{z,3}}{\partial t} = -\frac{1}{\tau} P_{z,3} - \frac{\epsilon_{\mathrm{r,s}} - \epsilon_{\mathrm{r},\infty}}{\epsilon_{\mathrm{r},\infty}\tau} P_{z,1} + \frac{(\epsilon_{\mathrm{r,s}} - \epsilon_{\mathrm{r},\infty})(\sigma_x + \sigma_y)}{\tau} E_z, \tag{A.46}$$

$$\frac{\partial P_{z,4}}{\partial t} = -\frac{\sigma}{\epsilon_0 \epsilon_{\mathrm{r},\infty}} P_{z,1} + \frac{\sigma(\sigma_x + \sigma_y)}{\epsilon_0} E_z, \tag{A.47}$$

$$\frac{\partial Q_x}{\partial t} = -\frac{\sigma_x}{\epsilon_0} Q_x + \frac{\mu_0 \mu_{\mathrm{r}} \sigma_x (\sigma_y - \sigma_x)}{\epsilon_0^2} H_x, \tag{A.48}$$

$$\frac{\partial Q_y}{\partial t} = -\frac{\sigma_y}{\epsilon_0} Q_y + \frac{\mu_0 \mu_{\mathrm{r}} \sigma_y (\sigma_x - \sigma_y)}{\epsilon_0^2} H_y. \tag{A.49}$$

Notice that Eqs. (A.44)–(A.49) contain no spatial derivatives and hence they are simply o.d.e.'s for $P_{z,1}$, $P_{z,2}$, $P_{z,3}$, $P_{z,4}$, Q_x, Q_y. Abarbanel and Gottlieb [12] pointed that the system using split-field PML terminating the computational domain was only *weakly* well-posed for the initial value problem. In contrast, the system (A.41)–(A.49), after dropping the undifferentiated terms, becomes the original 3×3 Maxwell system which is symmetric hyperbolic and therefore *strongly* well-posed.

It is straightforward to generalize this method for the medium having many Debye poles or Lorentz pole-pairs or for three-dimensional cases.

Appendix B. Non-dimensionalization of Maxwell's equations

Maxwell's equations are given as

$$\epsilon_0 \epsilon_{\mathrm{r},\infty} \frac{\partial \tilde{E}_z}{\partial \tilde{t}} = \frac{\partial \tilde{H}_y}{\partial \tilde{x}} - \frac{\partial \tilde{H}_x}{\partial \tilde{y}} - \left[\tilde{\sigma} + \epsilon_{\mathrm{r},\infty}(\tilde{\sigma}_x + \tilde{\sigma}_y) + \frac{\epsilon_0(\epsilon_{\mathrm{r,s}} - \epsilon_{\mathrm{r},\infty})}{\tilde{\tau}} \right] \tilde{E}_z + \tilde{P}_{z,1} + \tilde{P}_{z,2} - \tilde{P}_{z,3} - \tilde{P}_{z,4} \tag{B.1}$$

$$\mu_0 \mu_{\mathrm{r}} \frac{\partial \tilde{H}_x}{\partial \tilde{t}} = -\frac{\partial \tilde{E}_z}{\partial \tilde{y}} - \mu_0 \mu_{\mathrm{r}} \frac{\tilde{\sigma}_y - \tilde{\sigma}_x}{\epsilon_0} \tilde{H}_x + \tilde{Q}_x, \tag{B.2}$$

$$\mu_0 \mu_{\mathrm{r}} \frac{\partial \tilde{H}_y}{\partial \tilde{t}} = \frac{\partial \tilde{E}_z}{\partial \tilde{x}} - \mu_0 \mu_{\mathrm{r}} \frac{\tilde{\sigma}_x - \tilde{\sigma}_y}{\epsilon_0} \tilde{H}_y + \tilde{Q}_y, \tag{B.3}$$

$$\frac{\partial \tilde{P}_{z,1}}{\partial \tilde{t}} = -\frac{\epsilon_{\mathrm{r},\infty}}{\epsilon_0} \tilde{\sigma}_x \tilde{\sigma}_y \tilde{E}_z, \tag{B.4}$$

$$\frac{\partial \tilde{P}_{z,2}}{\partial \tilde{t}} = -\frac{1}{\tilde{\tau}} \tilde{P}_{z,2} + \frac{\epsilon_0(\epsilon_{\mathrm{r,s}} - \epsilon_{\mathrm{r},\infty})}{\tilde{\tau}^2} \tilde{E}_z, \tag{B.5}$$

$$\frac{\partial \tilde{P}_{z,3}}{\partial \tilde{t}} = -\frac{1}{\tilde{\tau}} \tilde{P}_{z,3} - \frac{\epsilon_{\mathrm{r,s}} - \epsilon_{\mathrm{r},\infty}}{\epsilon_{\mathrm{r},\infty}\tilde{\tau}} \tilde{P}_{z,1} + \frac{(\epsilon_{\mathrm{r,s}} - \epsilon_{\mathrm{r},\infty})(\tilde{\sigma}_x + \tilde{\sigma}_y)}{\tilde{\tau}} \tilde{E}_z, \tag{B.6}$$

$$\frac{\partial \tilde{P}_{z,4}}{\partial \tilde{t}} = -\frac{\tilde{\sigma}}{\epsilon_0 \epsilon_{\mathrm{r},\infty}} \tilde{P}_{z,1} + \frac{\tilde{\sigma}(\tilde{\sigma}_x + \tilde{\sigma}_y)}{\epsilon_0} \tilde{E}_z, \tag{B.7}$$

$$\frac{\partial \tilde{Q}_x}{\partial \tilde{t}} = -\frac{\tilde{\sigma}_x}{\epsilon_0}\tilde{Q}_x + \frac{\mu_0\mu_r\tilde{\sigma}_x(\tilde{\sigma}_y - \tilde{\sigma}_x)}{\epsilon_0^2}\tilde{H}_x, \tag{B.8}$$

$$\frac{\partial \tilde{Q}_y}{\partial \tilde{t}} = -\frac{\tilde{\sigma}_y}{\epsilon_0}\tilde{Q}_y + \frac{\mu_0\mu_r\tilde{\sigma}_y(\tilde{\sigma}_x - \tilde{\sigma}_y)}{\epsilon_0^2}\tilde{H}_y, \tag{B.9}$$

where ϵ_0 and μ_0 are the free space permittivity and permeability. The speed of light in free space is given by $c = (\epsilon_0\mu_0)^{-1/2}$. The characteristic impedance of free space is given by $Z = (\mu_0/\epsilon_0)^{1/2}$.

We non-dimensionalize the above set as follows:

$$x = \tilde{x}/L, \quad y = \tilde{y}/L, \quad t = c\tilde{t}/L, \tag{B.10}$$

$$H_x = Z\tilde{H}_x, \quad H_y = Z\tilde{H}_y, \quad E_z = \tilde{E}_z, \tag{B.11}$$

$$P_{z,i} = LZ\tilde{P}_{z,i}, \quad i = 1,2,3,4, \tag{B.12}$$

$$Q_x = L\tilde{Q}_x, \quad Q_y = L\tilde{Q}_y, \tag{B.13}$$

$$\sigma = LZ\tilde{\sigma}, \quad \sigma_x = LZ\tilde{\sigma}_x, \sigma_y = LZ\tilde{\sigma}_y, \tag{B.14}$$

$$\tau = c\tilde{\tau}/L, \tag{B.15}$$

L is a reference length associated with a given problem.

Thus, the non-dimensionalized form of Eqs. (B.1)–(B.9) is:

$$\epsilon_{r,\infty}\frac{\partial E_z}{\partial t} = \frac{\partial H_y}{\partial x} - \frac{\partial H_x}{\partial y} - \left[\sigma + \epsilon_{r,\infty}(\sigma_x + \sigma_y) + \frac{\epsilon_{r,s} - \epsilon_{r,\infty}}{\tau}\right]E_z + P_{z,1} + P_{z,2} - P_{z,3} - P_{z,4}, \tag{B.16}$$

$$\mu_r\frac{\partial H_x}{\partial t} = -\frac{\partial E_z}{\partial y} - \mu_r(\sigma_y - \sigma_x)H_x + Q_x, \tag{B.17}$$

$$\mu_r\frac{\partial H_y}{\partial t} = \frac{\partial E_z}{\partial x} - \mu_r(\sigma_x - \sigma_y)H_y + Q_y, \tag{B.18}$$

$$\frac{\partial P_{z,1}}{\partial t} = -\epsilon_{r,\infty}\sigma_x\sigma_y E_z, \tag{B.19}$$

$$\frac{\partial P_{z,2}}{\partial t} = -\frac{1}{\tau}P_{z,2} + \frac{\epsilon_{r,s} - \epsilon_{r,\infty}}{\tau^2}E_z, \tag{B.20}$$

$$\frac{\partial P_{z,3}}{\partial t} = -\frac{1}{\tau}P_{z,3} - \frac{\epsilon_{r,s} - \epsilon_{r,\infty}}{\epsilon_{r,\infty}\tau}P_{z,1} + \frac{(\epsilon_{r,s} - \epsilon_{r,\infty})(\sigma_x + \sigma_y)}{\tau}E_z, \tag{B.21}$$

$$\frac{\partial P_{z,4}}{\partial t} = -\frac{\sigma}{\epsilon_{r,\infty}}P_{z,1} + \sigma(\sigma_x + \sigma_y)E_z, \tag{B.22}$$

$$\frac{\partial Q_x}{\partial t} = -\sigma_x Q_x + \mu_r\sigma_x(\sigma_y - \sigma_x)H_x, \tag{B.23}$$

$$\frac{\partial Q_y}{\partial t} = -\sigma_y Q_y + \mu_r \sigma_y (\sigma_x - \sigma_y) H_y. \tag{B.24}$$

Appendix C. Riemann problem for dispersive media and the numerical flux equation (3.21)

The numerical flux equation (3.21) can be obtained by solving a one-dimensional Riemann problem with initial data indicated in Fig. 16. Mohammadian et al. [17] has obtained the numerical fluxes to the problem without source terms. Here, we will derive the fluxes to the case with source terms.

The weak solution [20,21] $\tilde{\mathbf{U}} = (\tilde{\mathbf{U}}^{(1)}, \tilde{\mathbf{U}}^{(1)})^{\mathrm{T}}$ to (3.12) and (3.13) satisfies for all functions $\boldsymbol{\psi}^{(1)} \in C_0^1(R \times [0, +\infty))^3$ and $\boldsymbol{\psi}^{(2)} \in C_0^1(R \times [0, +\infty))^6$

$$\int_0^\infty \int_R \left\{ \tilde{\mathbf{U}}^{(1)} \cdot \frac{\partial \boldsymbol{\psi}^{(1)}}{\partial t} + \nabla \boldsymbol{\psi}^{(1)} \cdot (\mathbb{A} \tilde{\mathbf{U}}^{(1)}) \right\} \mathrm{d}\zeta \, \mathrm{d}t + \int_R \tilde{\mathbf{U}}^{(1)}(\zeta, 0) \cdot \boldsymbol{\psi}^{(1)}(\zeta, 0) \, \mathrm{d}\zeta + \int_0^\infty \int_R \tilde{\mathbf{S}}^{(1)} \cdot \boldsymbol{\psi}^{(1)} \, \mathrm{d}\zeta \, \mathrm{d}t = 0, \tag{C.1}$$

$$\int_0^\infty \int_R \tilde{\mathbf{U}}^{(2)} \cdot \frac{\partial \boldsymbol{\psi}^{(2)}}{\partial t} \, \mathrm{d}\zeta \, \mathrm{d}t + \int_R \tilde{\mathbf{U}}^{(2)}(\zeta, 0) \cdot \boldsymbol{\psi}^{(2)}(\zeta, 0) \, \mathrm{d}\zeta + \int_0^\infty \int_R \tilde{\mathbf{S}}^{(2)} \cdot \boldsymbol{\psi}^{(2)} \, \mathrm{d}\zeta \, \mathrm{d}t = 0. \tag{C.2}$$

And it can be proved [20] that (C.1) and (C.2) imply that a piecewise C^1 function $\tilde{\mathbf{U}}$ is a solution of (3.12)–(3.14) if and only if the following two conditions are satisfied:

(i) $\tilde{\mathbf{U}}$ is a classical solution of $R \times [0, +\infty)$ in the domains where $\tilde{\mathbf{U}}$ is C^1;

(ii) $\tilde{\mathbf{U}}$ satisfies the Rankine–Hugoniot condition along a line of discontinuity with a speed s

$$(\tilde{\mathbf{U}}^{(1),-} - \tilde{\mathbf{U}}^{(1),+})s = \mathbb{A}^- \cdot \hat{\boldsymbol{n}} \tilde{\mathbf{U}}^{(1),-} - \mathbb{A}^+ \cdot \hat{\boldsymbol{n}} \tilde{\mathbf{U}}^{(1),+}, \tag{C.3}$$

where $^+$ and $^-$ denote the limits on each side of the line of discontinuity.

If there are no source terms, $\mathbf{S}^{(1)}$ and $\mathbf{S}^{(2)}$, piecewise constant solution in domain $\zeta < 0$ and domain $\zeta > 0$ can be obtained. Since $\mathbb{A} \cdot \hat{\boldsymbol{n}}$ is a constant matrix in both domains, we can construct the solution using the eigen-decomposition method [21]. It should be noted that an extra boundary condition is needed at $\zeta = 0$ for either domain, and these two boundary conditions are related by the Rankine–Hugoniot condition at $\zeta = 0$, i.e., $\mathbb{A}^- \cdot \hat{\boldsymbol{n}} \tilde{\mathbf{U}}^{(1),*} - \mathbb{A}^+ \cdot \hat{\boldsymbol{n}} \tilde{\mathbf{U}}^{(1),**} = 0$. (The meaning of * and ** are indicated in Fig. 16). With the source terms, the solution to this Riemann problem will not be piecewise constant anymore. But the lin-

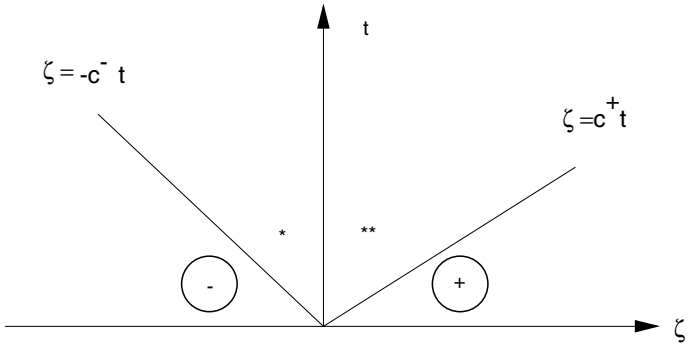

Fig. 16. Solution of the Riemann problem.

earity of the problem implies that the characteristics are still independent of the solution $\tilde{\mathbf{U}}$, and, thus, straight lines. However, we need to integrate along the characteristics to obtain the solution. Applying Rankine–Hugoniot conditions at the lines of discontinuity, we will get the solution in the whole domain $(-\infty,+\infty)\times[0,+\infty)$.

As $\tilde{\mathbf{U}}^{(2)}$ satisfies ordinary equations, and no spatial numerical fluxes are needed. So we just concentrate on solving $\tilde{\mathbf{U}}^{(1)}$. For simplicity, let $\mathbf{u}$ denote $\tilde{\mathbf{U}}^{(1)}$ and A denote $\mathbb{A}\cdot\hat{\boldsymbol{n}}$. Then, the one dimensional Riemann problem becomes

$$\frac{\partial}{\partial t}\mathbf{u}+\frac{\partial}{\partial\zeta}(A\mathbf{u})=\tilde{\mathbf{S}}^{(1)}, \tag{C.4}$$

$$\mathbf{u}(\zeta,0)=\begin{cases}\mathbf{u}^-, & \zeta<0,\\ \mathbf{u}^+, & \zeta>0,\end{cases} \tag{C.5}$$

where

$$A=\begin{cases}A^-, & \zeta<0,\\ A^+, & \zeta>0,\end{cases} \tag{C.6}$$

and

$$A^{\mp}=\begin{pmatrix}0 & n_y/\mu_{\mathrm{r}}^{\mp} & -n_x/\mu_{\mathrm{r}}^{\mp}\\ n_y/\epsilon_{\mathrm{r},\infty}^{\mp} & 0 & 0\\ -n_x/\epsilon_{\mathrm{r},\infty}^{\mp} & 0 & 0\end{pmatrix}. \tag{C.7}$$

$A^{\mp}$ has three different eigenvalues

$$\lambda_1^{\mp}=-c^{\mp},\quad \lambda_2^{\mp}=0,\quad \lambda_3^{\mp}=c^{\mp} \tag{C.8}$$

where $c^{\mp}=(\epsilon_{\mathrm{r},\infty}^{\mp}\mu_{\mathrm{r}}^{\mp})^{-1/2}$ is the speed of light in the medium. $A^{\mp}$ is diagonalizable with real eigenvectors, namely

$$A^{\mp}=R^{\mp}\Lambda^{\mp}(R^{\mp})^{-1} \tag{C.9}$$

where $\Lambda^{\mp}=\mathrm{diag}(\lambda_1^{\mp},\lambda_2^{\mp},\lambda_3^{\mp})$ is a diagonal matrix composed of $A^{\mp}$s eigenvalues, respectively. And $R^{\mp}=(\mathbf{r}_1^{\mp}|\mathbf{r}_2^{\mp}|\mathbf{r}_3^{\mp})$ is the matrix of right eigenvectors, and $(R^{\mp})^{-1}$ is $R^{\mp}$s inverse matrix

$$R^{\mp}=\begin{pmatrix}1 & 0 & 1\\ -n_yZ^{\mp} & n_x & n_yZ^{\mp}\\ n_xZ^{\mp} & n_y & -n_xZ^{\mp}\end{pmatrix},\quad (R^{\mp})^{-1}=\frac{1}{2}\begin{pmatrix}1 & -n_yY^{\mp} & n_xY^{\mp}\\ 0 & 2n_x & 2n_y\\ 1 & n_yY^{\mp} & -n_xY^{\mp}\end{pmatrix}, \tag{C.10}$$

where $Z^{\mp}=1/Y^{\mp}=(\mu^{\mp}/\epsilon^{\mp})^{1/2}$.

We define the new parameters $\mathbf{v}$,

$$\mathbf{v}=\begin{cases}(R^-)^{-1}\mathbf{u} & \text{if } \zeta<0,\\ (R^+)^{-1}\mathbf{u} & \text{if } \zeta>0.\end{cases} \tag{C.11}$$

In each of the region $\zeta<0$ or $\zeta>0$ along the pth characteristic, we have

$$\frac{\partial v_p}{\partial t}+\lambda_p\frac{\partial v_p}{\partial\zeta}=S_p,\quad p=1,2,3. \tag{C.12}$$

where S_p is the pth component of the source term $R^{-1}\tilde{\mathbf{S}}^{(1)}$, and

$$\lambda_p = \begin{cases} \lambda_p^- & \text{if } \zeta < 0, \\ \lambda_p^+ & \text{if } \zeta > 0. \end{cases} \tag{C.13}$$

The solution can be explicitly given by

$$v_p(\zeta, t) = v_p(\zeta - \lambda_p t, 0) + \int_0^t S_p \, \mathrm{d}\tilde{t} \tag{C.14}$$

where the integration is done along the characteristic $\tilde{\zeta} - \lambda_p \tilde{t} = \zeta - \lambda_p t$ with the initial value of $\mathbf{v}$ given as

$$\mathbf{v}(\zeta, 0) = \begin{cases} \mathbf{v}^-, & \zeta < 0 \\ \mathbf{v}^+, & \zeta > 0. \end{cases} = \begin{cases} (R^-)^{-1}\mathbf{u}^-, & \zeta < 0 \\ (R^+)^{-1}\mathbf{u}^+, & \zeta > 0. \end{cases} \tag{C.15}$$

From the definition of the numerical flux (3.18), we just need to compute the limit value $\lim_{t\to 0^+} \tilde{\mathbf{U}}^{(1)}(0^-, t)$ or $\lim_{t\to 0^+} \tilde{\mathbf{U}}^{(1)}(0^+, t)$.

Now consider a point E in Fig. 17. We can integrate along the line $\zeta - c^- t = \zeta_E - c^- t_E$ to get $v_3(\zeta_E^-, t_E)$, and the line $\zeta + c^+ t = \zeta_E + c^+ t_E$ to get $v_1(\zeta_E^+, t_E)$. (Note that $\zeta_E = 0$.)

From $v_3(0^-, t_E)$, $v_1(0^+, t_E)$ and the Rankine–Hugoniot condition at the characteristic $\zeta = 0$

$$A^+\mathbf{u}(0^+, t_E) - A^-\mathbf{u}(0^-, t_E) = 0, \tag{C.16}$$

we can get the unknown values $v_1(0^-, t_E)$ and $v_3(0^+, t_E)$.

Using Eqs. (C.9) and (C.11), Eq. (C.16) can be rewritten as

$$-c^- v_1(0^-, t_E)\mathbf{r}_1^- + c^- v_3(0^-, t_E)\mathbf{r}_3^- = -c^+ v_1(0^+, t_E)\mathbf{r}_1^+ + c^+ v_3(0^+, t_E)\mathbf{r}_3^+ \tag{C.17}$$

or

$$\begin{pmatrix} -c^- & c^- \\ c^- n_y Z^- & c^- n_y Z^- \\ -c^- n_x Z^- & -c^- n_x Z^- \end{pmatrix} \begin{pmatrix} v_1(0^-, t_E) \\ v_3(0^-, t_E) \end{pmatrix} = \begin{pmatrix} -c^+ & c^+ \\ c^+ n_y Z^+ & c^+ n_y Z^+ \\ -c^+ n_x Z^+ & -c^+ n_x Z^+ \end{pmatrix} \begin{pmatrix} v_1(0^+, t_E) \\ v_3(0^+, t_E) \end{pmatrix}. \tag{C.18}$$

From Eq. (C.18), we can solve

$$\begin{pmatrix} v_1(0^-, t_E) \\ v_3(0^+, t_E) \end{pmatrix} = \begin{pmatrix} -\frac{Z^- - Z^+}{Z^- + Z^+} v_3(0^-, t_E) + \frac{2Z^+}{Z^- + Z^+} \frac{c^+}{c^-} v_1(0^+, t_E) \\ \frac{Z^- - Z^+}{Z^- + Z^+} v_1(0^+, t_E) + \frac{2Z^-}{Z^- + Z^+} \frac{c^-}{c^+} v_3(0^-, t_E) \end{pmatrix}. \tag{C.19}$$

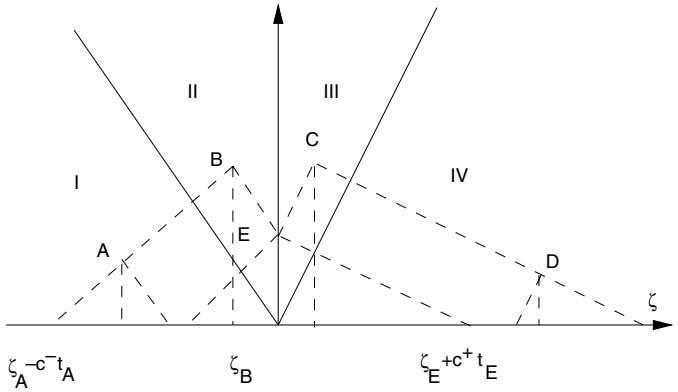

Fig. 17. Construction of solution to Riemann problem at (ζ, t).

From Eqs. (C.14) and (C.15), we have

$$v_1(0^+,t_E)=v_1^+ + \int_0^{t_E} S_1\,\mathrm{d}t, \quad v_3(0^-,t_E)=v_3^- + \int_0^{t_E} S_3\,\mathrm{d}t. \tag{C.20}$$

Let $t_E \to 0^+$, we have

$$\lim_{t_E\to 0^+} v_1(0^+,t_E)=v_1^+, \quad \lim_{t_E\to 0^+} v_3(0^-,t_E)=v_3^-. \tag{C.21}$$

From Eq. (C.16) and the definition of the numerical flux (3.18), we can get the numerical flux

$$\mathbf{h}(\mathbf{u}^-,\mathbf{u}^+)=\lim_{t_E\to 0^+} A^+\mathbf{u}^-(0^+,t_E)=\lim_{t_E\to 0^+}(-c^+v_1(0^+,t_E)\mathbf{r}_1^+ + c^+v_3(0^+,t_E)\mathbf{r}_3^+). \tag{C.22}$$

Substituting $v_3(0^+,t_E)$ in Eq. (C.19) into the Eq. (C.22) gives

$$\mathbf{h}(\mathbf{u}^-,\mathbf{u}^+)=\lim_{t_E\to 0^+}\left[-c^+v_1(0^+,t_E)\mathbf{r}_1^+ + c^+\frac{Z^- - Z^+}{Z^- + Z^+}v_1(0^+,t_E)\mathbf{r}_3^+ + c^-\frac{2Z^-}{Z^- + Z^+}v_3(0^-,t_E)\mathbf{r}_3^+\right]. \tag{C.23}$$

Using Eqs. (C.21) and (C.23), we get

$$\mathbf{h}(\mathbf{u}^-,\mathbf{u}^+)=-c^+v_1^+\mathbf{r}_1^+ + c^+\frac{Z^- - Z^+}{Z^- + Z^+}v_1^+\mathbf{r}_3^+ + c^-\frac{2Z^-}{Z^- + Z^+}v_3^-\mathbf{r}_3^+. \tag{C.24}$$

Substituting v_1^+ and v_3^- in Eq. (C.15) and $\mathbf{r}_1^+$ and $\mathbf{r}_3^+$ in Eq. (C.10) into Eq. (C.24) gives

$$\mathbf{h}(\mathbf{u}^-,\mathbf{u}^+)=\begin{pmatrix} -\frac{\left[Z(n_xH_y-n_yH_x)-E_z\right]^- + \left[Z(n_xH_y-n_yH_x)+E_z\right]^+}{Z^-+Z^+} \\ n_y\frac{\left[YE_z-(n_xH_y-n_yH_x)\right]^- + \left[YE_z+(n_xH_y-n_yH_x)\right]^+}{Y^-+Y^+} \\ -n_x\frac{\left[YE_z-(n_xH_y-n_yH_x)\right]^- + \left[YE_z+(n_xH_y-n_yH_x)\right]^+}{Y^-+Y^+} \end{pmatrix}, \tag{C.25}$$

which proves Eq. (3.21). And a similar method applying to the three dimensional Maxwell's equations gives Eq. (3.20).

References

[1] D.A. Kopriva, S.L. Woodruff, M.Y. Hussaini, Computation of electromagnetic scattering with a non-conforming discontinuous spectral element method, Int. J. Numer. Meth. Eng. 53 (2002) 105.

[2] B. Cockburn, S. Hou, C.W. Shu, Tvb Runge–Kutta local projection discontinuous Galerkin finite element method for conservation laws iv: The multidimensional case, Math. Comp. 54 (1990) 545.

[3] J.S. Hesthaven, T. Warburton, High-order/Spectral methods on unstructured grids I. time-domain solution of Maxwell's equations, NASA/CR-20010210836 ICASE Report, No. 2001-6, ICASE Mail Stop 132C NASA Langley Research Center Hampton, VA 23681-2199 (March 2001).

[4] T. Warburton, Application of the discontinuous Galerkin method to Maxwell's equations using unstructured polymorphic *hp*-finite elements, in: International Symposium on Discontinuous Galerkin Methods, 1999.

[5] B. Szabo, I. Babuska, Finite Element Analysis, Wiley, New York, 1991.

[6] A. Bayliss, E. Turkel, Radiation boundary conditions for wave-like equations, Comm. Pure Appl. Math. 23 (1980) 707.

[7] B. Enquist, A. Majda, Absorbing boundary conditions for the numerical solution of waves, Math. Comp. 31 (1977) 629.

[8] D. Givoli, Nonreflecting boundary conditions, J. Comput. Phys. 94 (1991) 1.

[9] J.P. Berenger, A perfectly matched layer for the absorption of electromagnetic waves, J. Comput. Phys. 114 (1994) 185.

[10] Z.S. Sacks, D.M. Kingsland, R. Lee, J.-F. Lee, A perfectly matched anisotropic absorber for use as an absorbing boundary condition, IEEE Trans. Antennas Propagat. 43 (Dec.) (1995) 1460.

[11] R. Ziolkowski, Time derivative Lorentz model based absorbing boundary condition, IEEE, Trans. Antennas Propagat. 45 (1997) 1530.
[12] S. Abarbanel, D. Gottlieb, On the construction and analysis of absorbing layers in CEM, Appl. Numer. Math. 27 (4) (1998) 331.
[13] A. Taflove, S.C. Hagness, Computational Electromagnetics: The Finite-Difference Time-Domain Method, second ed., Artech House, Boston/Lodon, 2000.
[14] T.G. Moore, J.G. Blaschak, A. Taflove, G.A. Kriegsmann, Theory and application of radiation boundary operators, IEEE Trans. Antennas Propag. 36 (1988) 1797.
[15] N. Bloembergen, Nonlinear Optics, W.A. Benjamin, New York, 1965.
[16] S.Z. Deng, W. Cai, Numerical modeling of optical coupling by whispering gallery modes between microcylinders, J. Comput. Phys., November, 2003 (submitted).
[17] A.H. Mohammadia, V. Shankar, W.F. Hall, Computation of electromagnetic scattering and radiation using a time domain finite volume discretization procedure, Comput. Phys. Comm. 68 (1991) 175.
[18] K. Umashankar, A. Taflove, Computational Electrodynamics, Artech House, Boston, 1993.
[19] Q.H. Liu, G.X. Fan, Simulations of GPR in dispersive media using a frequency-dependent PSTD algorithm, IEEE Trans. Geosci. Remote Sensing 37 (5) (1999) 2317.
[20] E. Godlewski, P.A. Raviart, Numerical Approximation of Hyperbolic Systems of Conservation Laws, Springer, New York, 1996.
[21] R.J. LeVeque, Numerical Methods for Conservation Laws, Birkhauser, Basel/Boston, 1992.
[22] B. Cockburn, F. Li, C.-W. Shu, Locally divergence-free discontinuous Galerkin methods for the Maxwell equations, J. Comput. Phys. 194 (2004) 588.
[23] T. Warburton, L. Pavarino, J.S. Hestheven, A pseudospectral scheme for incompressible Navier–Stokes using unstructured nodal elements, J. Comput. Phys. 164 (1) (2000) 1.